VOLUME 22, 1960/61, No. 6 pp. 181-216 Published 14th March 1961

Philips Technical Review

DEALING WITH TECHNICAL PROBLEMS
RELATING TO THE PRODUCTS, PROCESSES AND INVESTIGATIONS OF
THE PHILIPS INDUSTRIES

WAVEGUIDE EQUIPMENT FOR 2 mm MICROWAVES

II. MEASURING SET-UPS

621.372.8:621.317.3

by C. W. van ES, M. GEVERS and F. C. de RONDE.

In Part I of this article, a review was given of the equipment developed by Philips for 2 mm microwaves. Part II below contains a description of some measuring set-ups in which the use of the components discussed are considered in more detail; in addition, some components which were not considered in Part I are also described.

The first two set-ups discussed are for the measurement of the losses and the impedances of microwave components. The third set-up is a microwave gas spectrometer by means of which the absorption lines in gases can be experimentally determined.

When designing components for a new frequency range, the microwave technician requires good measuring equipment in order to investigate the properties of the developed components. In this context, his preference will be for measuring instruments which do not need to be calibrated, i.e. instruments which are "absolute". The rotary attenuator is one such instrument. This latter can be used for the measurement of attenuations such as the dissipative loss in microwave components, which will later be discussed. The rotary attenuator itself was treated in Part I of this article [1]); likewise, the variable impedance with which reflection coefficients can be measured. This instrument is also absolute as far as the modulus of the reflection coefficient is concerned. It is used in the second measuring set-up discussed below for measuring the reflection coefficient of an unknown impedance in a bridge circuit (with a hybrid T as the bridge element). Here, the variable impedance serves as a reference impedance.

The third measuring set-up to be discussed is for the investigation of absorption spectra in gases. An example is carbonyl-sulphide gas (COS), which exhibits absorption at about 146 Gc/s. If the gas is irradiated at the correct frequency, the energy supplied allows the COS molecules to move to a higher rotational level. This transition is accompanied by absorption. The frequency at which absorption occurs can be determined with the set-up to be described.

Measurement of the dissipative loss in microwave components

When a microwave component is inserted in a waveguide set-up which has been matched to both the load and generator sides, the losses will in general increase. This increase, which is called "insertion loss", is caused partly by reflections and partly by dissipation in the four-terminal network constituted by the inserted component. Reflection and dissipation are both characteristic properties of a four-terminal network. The dissipative loss can be measured in the manner now to be described; the reflective loss is derived from an impedance measurement using a second set-up which will be dealt with presently.

It is almost always desired to keep the dissipative loss as small as possible, and for that reason an effort has been made to keep the length of our components to a minimum. The need for short components becomes more evident as the frequency increases, since the loss per unit length increases as the $\frac{3}{2}$ power of the frequency. As mentioned in Part I, the claw flange with its associated lock ring is one of the devices used to achieve short constructions

[1]) C. W. van Es, M. Gevers and F. C. de Ronde, Waveguide equipment for 2 mm microwaves, I. Components, Philips tech. Rev. **22**, 113-125, 1960/61 (No. 4).

with correspondingly low dissipative losses. Moreover, at high frequencies the surface roughness has a considerable influence: the higher the frequency, and therefore the smaller the depth of penetration, the greater the resistance which irregularities and impurities will offer to the current.

The dissipative loss can be determined by two power measurements, one *with* the component being investigated in the set-up and one *without* it. The power can be measured by a water calorimeter; this is an absolute instrument but is cumbersome to use. In its place, use can be made of a thermistor, i.e. a thermal detector, which has been calibrated by a water calorimeter or (somewhat less accurately) by DC [2]). Also, a crystal detector (*fig. 1*) with a DC meter can be used as a power indicator. The crystal is a more or less square-law detector, so that the deflection of the meter is approximately proportional to the microwave power. The dissipation loss can be found from the ratio of the readings given by the two power measurements. Use of the rotary attenuator has the advantage that the two measurements can be made at the same crystal power, the measurements then being completely independent of the detection characteristic. The difference in position

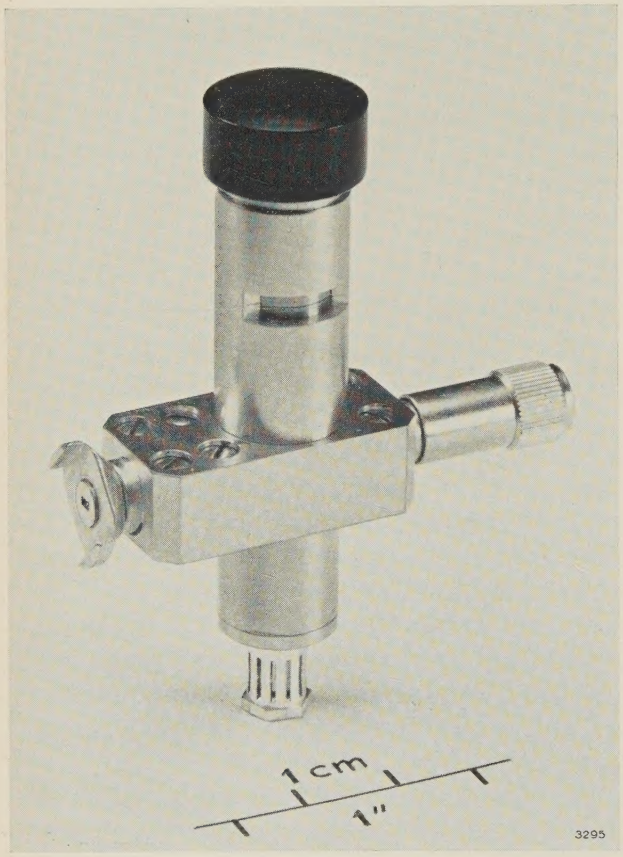

Fig. 1. Crystal detector for 2 mm waves. Left, claw flange, right, shorting plunger. The differential screw which is used to bring the silicon crystal into contact with the catswhisker is situated beneath the black cap; the displacement can be monitored through the window. Below: the coaxial connection for the millivoltmeter. The sensitivity is better than 10 mV per mW.

[2]) See Philips tech. Rev. **21**, 228 (Note [7])), 1959/60 (No. 8).

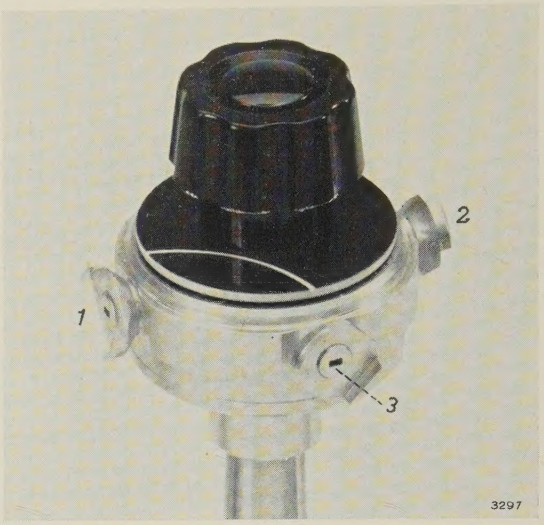

Fig. 2. Waveguide switch for 2 mm wavelength. A rotatable piece of waveguide, in the form of a quadrant, connects waveguide *3* to waveguide *1* in one position of the switch, and waveguide *3* to waveguide *2* in the other position. The standing-wave ratio is less than 1.02.

of the rotary attenuator when the component is present from that when it is removed from the set-up thus gives the dissipative loss directly.

In these measurements, it is desirable to be able to switch rapidly from one condition to another since, in the interim period, the supplied power may vary for all sorts of reasons: the output power from the klystron, the conversion of the frequency multiplier and the sensitivity of the detector are subject to irregular fluctuations. Rapid switching-over is made possible by means of a waveguide switch (*fig. 2*). This contains a rotatable part consisting of a curved waveguide of quadrant form so that, according to requirements, a connection can be made between the waveguides *3* and *1* or *3* and *2*. It will be clear that particularly high demands are placed upon the mechanical construction and finish, in order to obtain a reproducible connection with a very low reflection coefficient (e.g. $|R|$ smaller than 0.01) between the rotatable and fixed parts of the waveguide.

The circuit with crystal detector and waveguide switch is reproduced in *fig. 3*; a photo of the whole set-up is given in *fig. 4* and a photo of the 2 mm part in *fig. 5*. Two branches are connected to the waveguide switch *S*. One consists of the component to be measured, in this case a piece of waveguide of

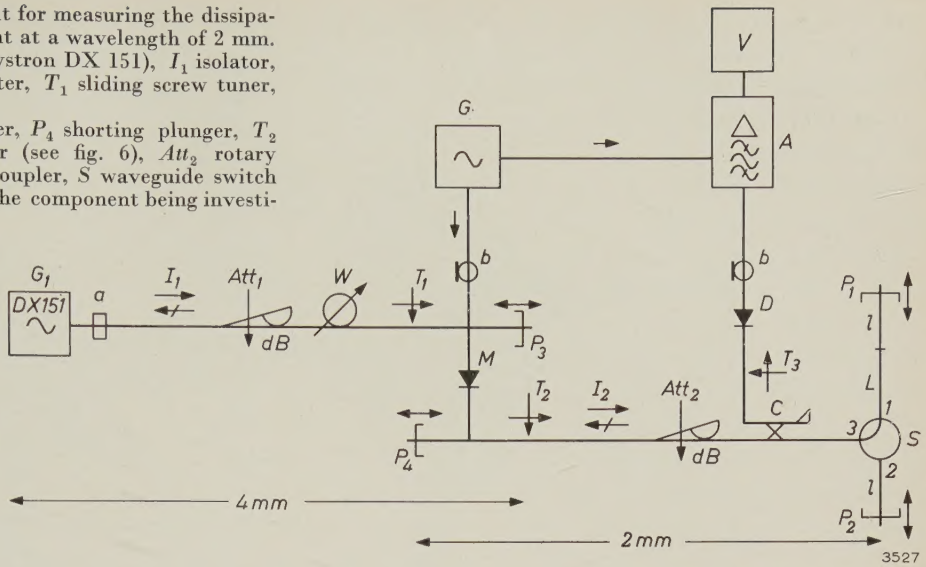

Fig. 3. Block diagram of the circuit for measuring the dissipative loss in a microwave component at a wavelength of 2 mm. *4 mm part*: G_1 generator (reflex klystron DX 151), I_1 isolator, Att_1 vane attenuator, W wavemeter, T_1 sliding screw tuner, P_3 shorting plunger. *2 mm part*: M frequency multiplier, P_4 shorting plunger, T_2 pivoting screw tuner, I_2 isolator (see fig. 6), Att_2 rotary attenuator, C rotary directional coupler, S waveguide switch (see fig. 2). Branch *1* consists of the component being investigated (length L) combined with a line of length l adjustable with plunger P_1. Branch *2* consists of a similar length l adjustable with plunger P_2. T_3 pivoting screw tuner. D detector (see fig. 1). *Other equipment*: G generator (8 kc/s) for synchronous detection, A selective amplifier, V millivoltmeter. The sign *a* means "rectangular waveguide" and the sign *b* means "coaxial line".

length L terminated at a distance l from the flange by a shorting plunger P_1. The other branch is terminated directly by a plunger P_2, this latter being adjusted to the same distance l. By means of the waveguide switch, either the branch $L + l$ or the branch l can thus be connected to the rest of the circuit. The circuit contains, in addition to a rotary attenuator, a rotary directional coupler C — a component described in Part I. The rotary directional coupler is used to measure the reflected wave which comes back from the branch switched in by S.

The measurement of the dissipative loss is carried out as follows. With the waveguide switch in position *1*, adjustments are made until the meter V shows full-scale deflection, and the rotary attenuator is set to zero. This done, S is switched to position *2*, i.e. to the opposite branch from that carrying the component to be measured. The attenuation will

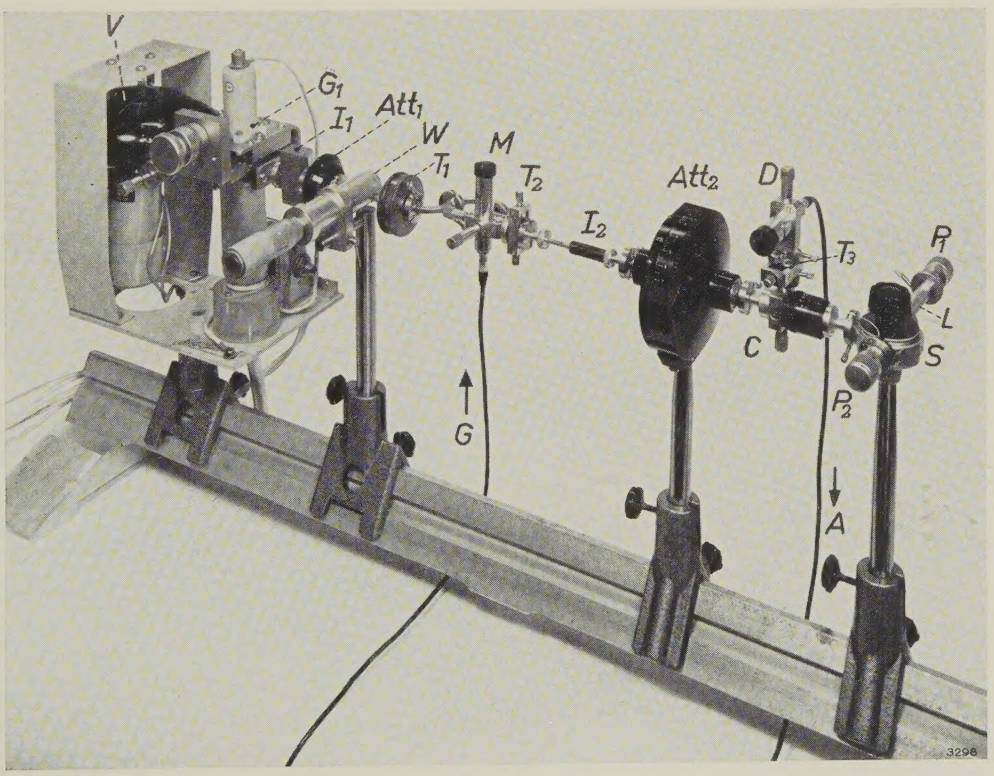

Fig. 4. Set-up for measuring the dissipative loss in components at a wavelength of 2 mm (refer to the diagram in fig. 3). V cooling fan for the reflex klystron. Notation otherwise as in fig. 3.

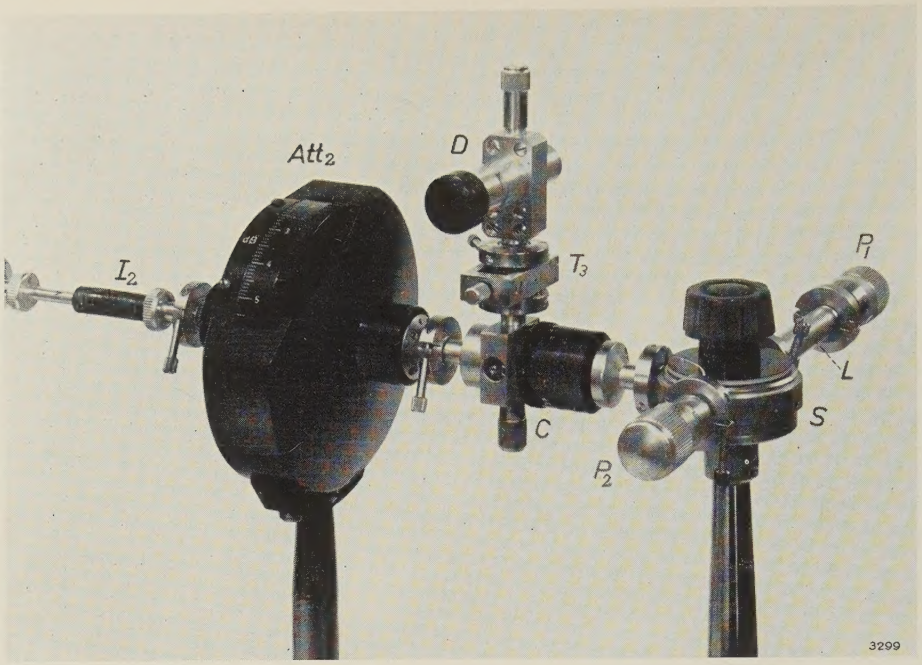

Fig. 5. The 2 mm part of the set-up reproduced in fig. 4. Notation as in fig. 3.

then be less, hence the reflected wave stronger and the meter will tend to deflect further. Now, using the rotary attenuator, the signal is attenuated sufficiently to restore the meter to its original deflection. We then read off from the rotary attenuator the indicated attenuation. Half this attenuation gives the dissipation in the component (half, since the wave traverses the length L of the component twice).

In order to make the measurement as accurate as possible, a few precautions must be taken, one of which is to include a directional isolator.

Looking towards the generator, the transmission line will not generally be reflection-free. For this reason, on displacing the plunger P_1 or P_2, the deflection of the meter will vary. In order to keep this effect as small as possible, an isolator is connected between the attenuator and the multiplier (I_2 in fig. 3). This device, whose operation depends on the Faraday effect [3]), is depicted in *fig. 6*. However, even with these precautions some reflection will remain so that, in order to adjust the meter to the maximum or minimum deflection, the plungers P_1 and P_2 must both be adjustable.

At the beginning of the measurement, and before the component of length L has been inserted in one of the branches, it must be ascertained that the two branches (length l) are identical, i.e. that, for both positions of the waveguide switch, the meter deflections are the same. When the component L is subsequently fitted into the branch l, a small phase change will generally appear (unless the length L is precisely a whole multiple of $\frac{1}{2}\lambda_g$, where λ_g is the wavelength in the guide). This phase change can be corrected by adjusting the plunger P_1. In its turn, this adjustment causes some change in the dissipative loss, but only to a negligibly small degree.

Since the use of a directional coupler means that *reflections* from the component are also measured, it must first be ascertained that these are indeed negligibly small. If this is not the case, the reflection must first be compensated.

The measures taken make a very accurate measurement possible. The circuit described is particularly suited to the measurement of losses in sections of waveguide and residual losses in components, e.g. the losses in a vane attenuator (see Part I) in the zero position. With this method, losses of the order of 0.1 dB can easily be measured.

The dissipative loss in the components discussed in Part I was measured with the circuit of fig. 3. This does not, of course, mean that the method is only suitable for measurements on microwave components; it can be used equally well for measuring attenuations caused by any sort of physical

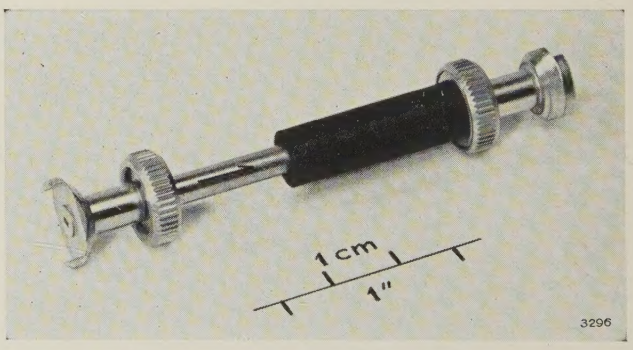

Fig. 6. Isolator for 2 mm wavelength, based on the Faraday effect [3]). The black rings are ferroxdure magnets. Attenuation in the forward direction (in the direction of the arrow): 2 dB; in the reverse direction: 15 dB.

[3]) H. G. Beljers, The application of ferroxcube in unidirectional waveguides and its bearing on the principle of reciprocity, Philips tech. Rev. **18**, 158-166, 1956/57.

phenomena. It is, for example, very useful for measuring the absorption in superconductors [4]).

Impedance measurements using the bridge method

In general, an impedance reflects some of the applied microwave energy when the impedance differs from the characteristic impedance of the line. A measure of this "mismatch" is either the standing-wave ratio or the reflection coefficient [5]). In order to determine the impedance by means of the standing-wave ratio, a standing-wave detector is necessary. However, it is extremely difficult to make a standing-wave detector for millimetre waves with reasonable accuracy. A more direct measurement of the impedance is possible by inserting it in a bridge circuit and comparing it with a standard impedance. The variable impedance discussed in Part I can serve this latter purpose. This instrument is absolute and the value of the reflection coefficient of the unknown impedance can be read off directly.

The circuit is reproduced in *fig. 7*. It consists of a 4 mm and a 2 mm part, the latter containing a hybrid T (see Part I), *HT*, as the bridge element. The input arm *1* of the T is connected to the frequency multiplier *M* via a pivoting screw tuner T_1. On the arm *4*, via another pivoting screw tuner T_3, a crystal detector *D* is connected, and on the arms *2* and *3* the variable impedance Z_V and the unknown impedance Z_3, respectively. The latter consists of a pivoting screw tuner T_2 in conjunction with a matched load. Using this assembly, any required impedance can be made up.

The energy coming from the multiplier divides in the hybrid T into two equal parts, which travel along the arms *2* and *3*. Z_3 will cause a certain amount of reflection in arm *3*; the reflected wave returns to the branching point of the hybrid T and distributes itself over the arms *1* and *4*. If the reflection from Z_V is now made equal in phase and amplitude to the reflection from Z_3, then a reflected wave of equal magnitude will likewise be split into two equal parts at the branching point and travel along the arms *1* and *4*. As explained in Part I, the geometric configuration is such that the waves issuing from the arms *2* and *3* cancel each other in arm *4;* therefore, the detector *D* receives no signal and the meter does not deflect. This is thus an indication that $Z_V = Z_3$, and the modulus of the reflection coefficient can be directly read off on the variable impedance, whilst its argument can be rapidly determined (see Part I, page 121).

A detail photo of the 2 mm part of this set-up is shown in *fig. 8*.

The sensitivity of this method is very high. Another property of the bridge circuit is that the sensitivity is considerably greater if the measurement is made after the bridge has been slightly unbalanced. This property is useful in the measurement of very weak reflections, such as those which occur at flanges, when values of $|R|$ less than 0.01 can still be fairly reliably measured. For this purpose, one arm of the hybrid T is terminated by a matched load and

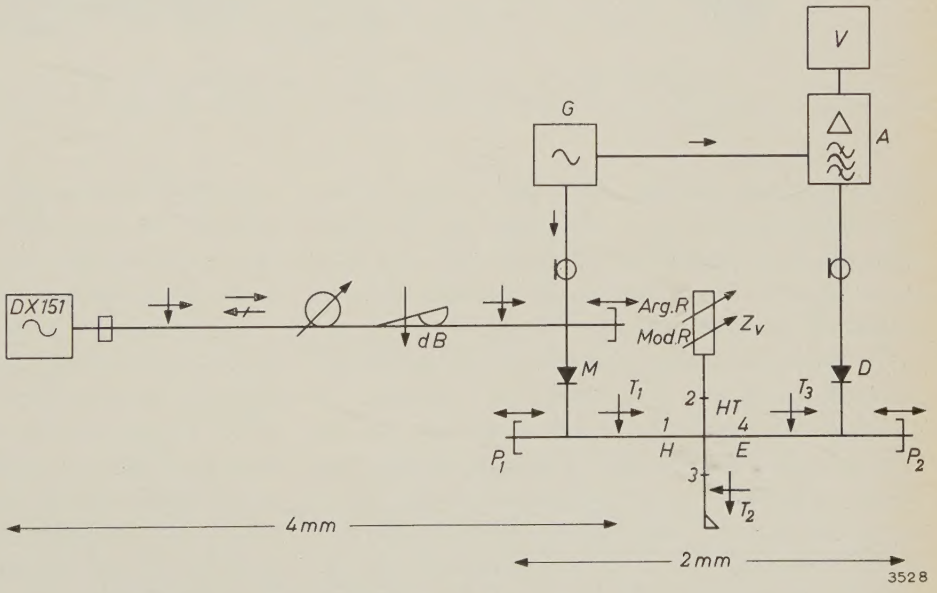

Fig. 7. Block diagram of the circuit for measuring the reflection coefficient of impedances at a wavelength of 2 mm.
4 mm part, from left to right: generator, sliding screw tuner, isolator, wavemeter, vane attenuator, sliding screw tuner, shorting plunger.
2 mm part: *M* frequency multiplier, P_1 shorting plunger, T_1 pivoting screw tuner, *HT* hybrid T, Z_V variable impedance, T_2 pivoting screw tuner (with matched load), T_3 pivoting screw tuner, P_2 shorting plunger, *D* detector.
Other equipment: *G* generator (8 kc/s), *A* selective amplifier (tuned to the frequency of *G*), *V* millivoltmeter.

[4]) M. A. Biondi and M. P. Garfunkel, Millimeter wave absorption in superconducting aluminum, I and II, Phys. Rev. **116**, 853-867, 1959 (No. 4).

[5]) For the relationships between the quantities impedance, reflection coefficient and standing-wave ratio, see e.g. A. E. Pannenborg, A measuring arrangement for waveguides, Philips tech. Rev. **12**, 15-24, 1950/51.

a small reflection is introduced in the arm containing the variable impedance, so that the bridge is slightly out of balance. By altering the $|R|$ of the variable impedance by a certain amount with respect to the adjusted value (readable upon the scale "mod R", see fig. 16 of Part I), a specific variation in the deflection of the meter is obtained. The introduction of a flange coupling between the hybrid T shown in Part I, as far as the hybrid T is concerned the accuracy is determined solely by the mechanical construction and the finish. In the variable impedance, still other factors play a part. The detrimental influence of all these factors upon the accuracy are particularly noticeable in the two extreme positions, mod $R = 1$ and mod $R = 0$. In the latter position, there is always some residual reflection,

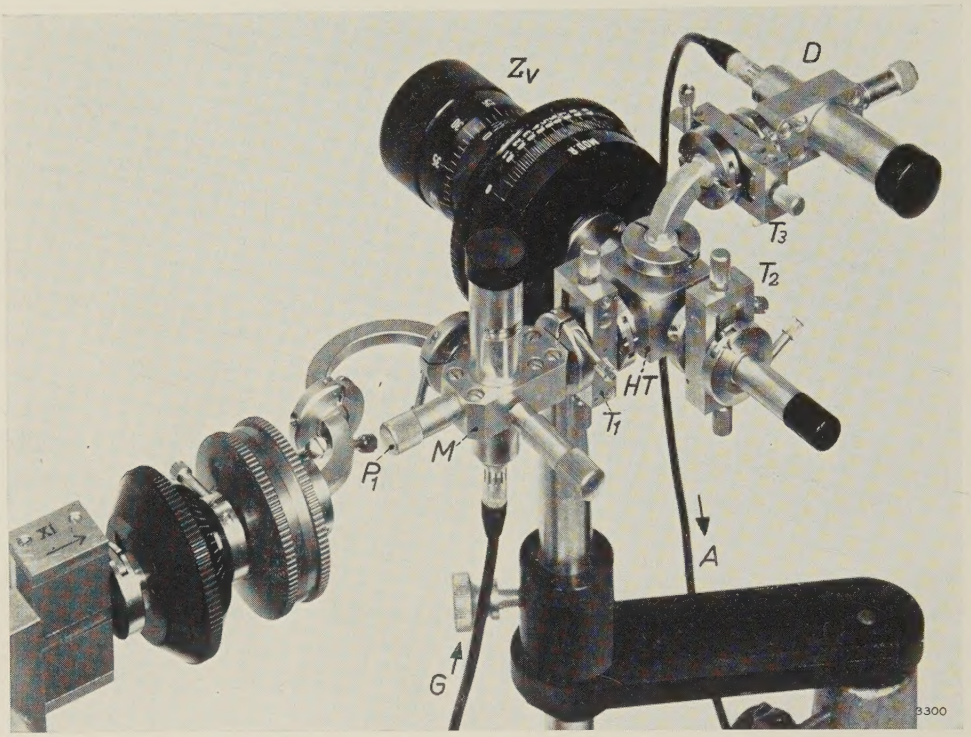

Fig. 8. The 2 mm part of the set-up shown in the diagram of fig. 7. Notation as in the latter. At the extreme left, a few 4 mm components: isolator, vane attenuator and sliding screw tuner.

and the matched load likewise causes a change in the deflection. The reflection coefficient can be found from the two changes in deflection. The fact that there are still other reflections of the same order of magnitude as those which are being measured, actually makes the measurement somewhat more complicated than is here described. It is necessary, for example, to compensate as well as possible for the reflections at other flange connections in the arms and for reflections at the transition, and the reflection at the matched load can no longer be neglected. When reasonably accurate measurements are required of very small reflection coefficients such as occur at claw-flange couplings, all this must be taken into account.

The accuracy with which the reflection coefficient of an impedance can be determined is dependent upon the quality of two components: *a*) the hybrid T and *b*) the variable impedance. As has already been namely at the transition from the rectangular waveguide to the circular waveguide. If extremely accurate measurement is required, this residual reflection must be neutralized by means of a tuner.

In the maximum reflection position, $|R|$ is not quite 1 because of the losses in the waveguide. Here, again, is an advantage of the bridge circuit, in that these losses can be compensated by inserting between the impedance Z_3 and the hybrid T a section of waveguide which causes identical losses. For this purpose, the variable impedance is set to the position mod $R = 1$ and, in the other arm of the hybrid T, Z_3 is replaced by a short-circuited piece of waveguide of such length that, by adjustment of the phase, equilibrium can be established. Having balanced the bridge in this way for mod $R = 1$, we can then determine the dissipative loss α in components having low reflection. For this purpose the component is connected between the short-circuit

and the added piece of waveguide. If balance is subsequently re-established, then:

$$a = -10 \log |R| \text{ dB}.$$

Thus, the dissipative loss in microwave components can be determined by the method just described as well as by the circuit of fig. 3. The measurement of large losses is, in both cases, limited by reflections.

Measurement of an absorption line of COS at 2 mm

The binding forces existing between particles which together form a "system" (such as between the atoms in a molecule, between the nucleus and the electrons in an atom, between the protons and the neutrons in an atomic nucleus) give rise to a series of energy states which the system can occupy. On absorbing electromagnetic energy of certain frequencies, such a system can change from a given energy state to one of higher energy. A transition from the n^{th} to the $(n+1)^{\text{th}}$ energy level is made possible by absorption of radiation whose frequency ν is proportional to the energy difference $E_{n+1} - E_n$ between the two levels:

$$\nu = \frac{E_{n+1} - E_n}{h}.$$

Here, h is Planck's constant ($= 6.6 \times 10^{-34}$ joule seconds). The energy levels E_n are determined by the nature of the forces and the kinds of particles. Thus, absorption in the gamma ray region is caused by changes of state within the atomic nucleus; absorption in the optical region is predominantly concerned with the binding forces between nuclei and electrons, and absorption in the infra-red and microwave regions are related to the force which the atoms of the molecule exert upon one another.

Thus, microwave spectroscopy can provide information concerning the chemical bonds in molecules (vibrational and rotational states). Here, infra-red spectroscopy is also important, but spectroscopy in the microwave region has the advantages that the radiation is purely monochromatic and that the sensitivity, the accuracy of determination of the absorption frequencies and the resolving power are greater. The latter is such that fine and hyperfine structures can be observed, enabling conclusions to be drawn concerning the behaviour of the nuclei of individual atoms. For further particulars the reader is referred to the literature [6]).

The third set-up, now to be discussed, is a microwave gas spectrometer used for determining the rotational spectra of gas molecules. The diagram of the circuit is reproduced in *fig. 9*. The main components in the 2 mm part — shown separately in *fig. 10* — are a gas cell *GC* and a 2 mm crystal detector D_1. The gas cell consists of a piece of 8 mm waveguide (this being used since it has a greater volume and smaller wall-losses per unit length) with at each end a transition to 2 mm guide. The

[6]) See, for example: W. Gordy, W. V. Smith and R. F. Trambarulo, Microwave spectroscopy, Wiley, New York 1957.
D. J. E. Ingram, Spectroscopy at radio and microwave frequencies, Butterworth's Scientific Publications, London 1955.
C. A. Burrus, Stark effect from 1.1 to 2.6 millimeters wavelength: PH_3, PD_3, DI, and CO, J. chem. Phys. **28**, 427-429, 1958.
M. Cowan and W. Gordy, Precision measurements of millimeter and submillimeter wave spectra: DCl, DBr, and DI, Phys. Rev. **111**, 209-211, 1958.

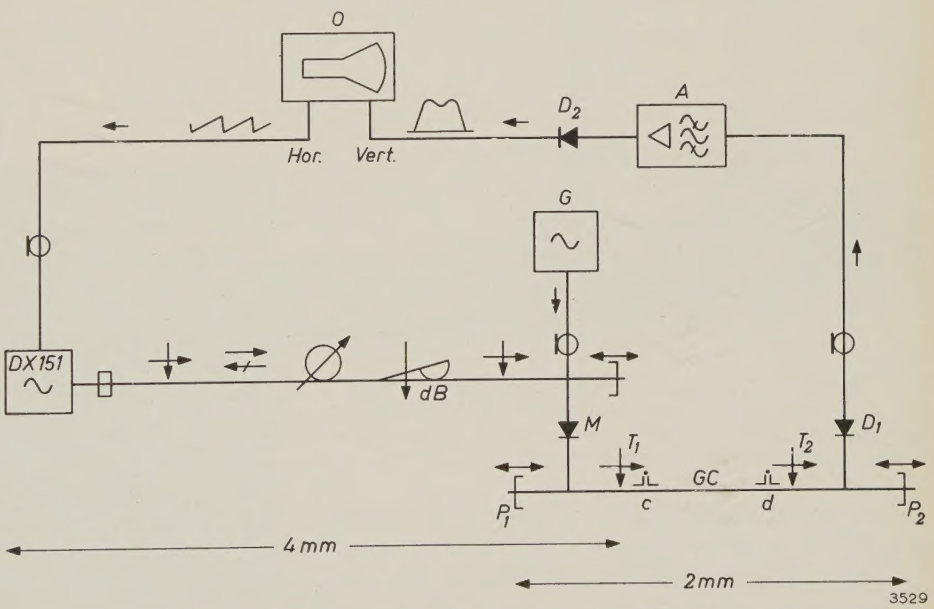

Fig. 9. Block diagram of the circuit for measuring the absorption line of carbonyl sulphide at about 146 Gc/s.
4 mm part, from left to right: generator, sliding screw tuner, isolator, wavemeter, vane attenuator, sliding screw tuner, shorting plunger.
2 mm part: *M* frequency multiplier, P_1 shorting plunger, T_1 pivoting screw tuner, *GC* gas cell (with mica windows *c* and *d*), T_2 pivoting screw tuner, P_2 shorting plunger, D_1 detector.
Other equipment: *G* generator (45 kc/s) which amplitude-modulates the 2 mm wave, *A* selective amplifier tuned to the frequency of *G*, D_2 detector, *O* oscilloscope. The sawtooth time-base voltage of *O* frequency-modulates the 4 mm generator. The form of the detected microwave is indicated at the input of *A*; the form of the signal after low-frequency detection by D_2 is shown at the input of *O*.

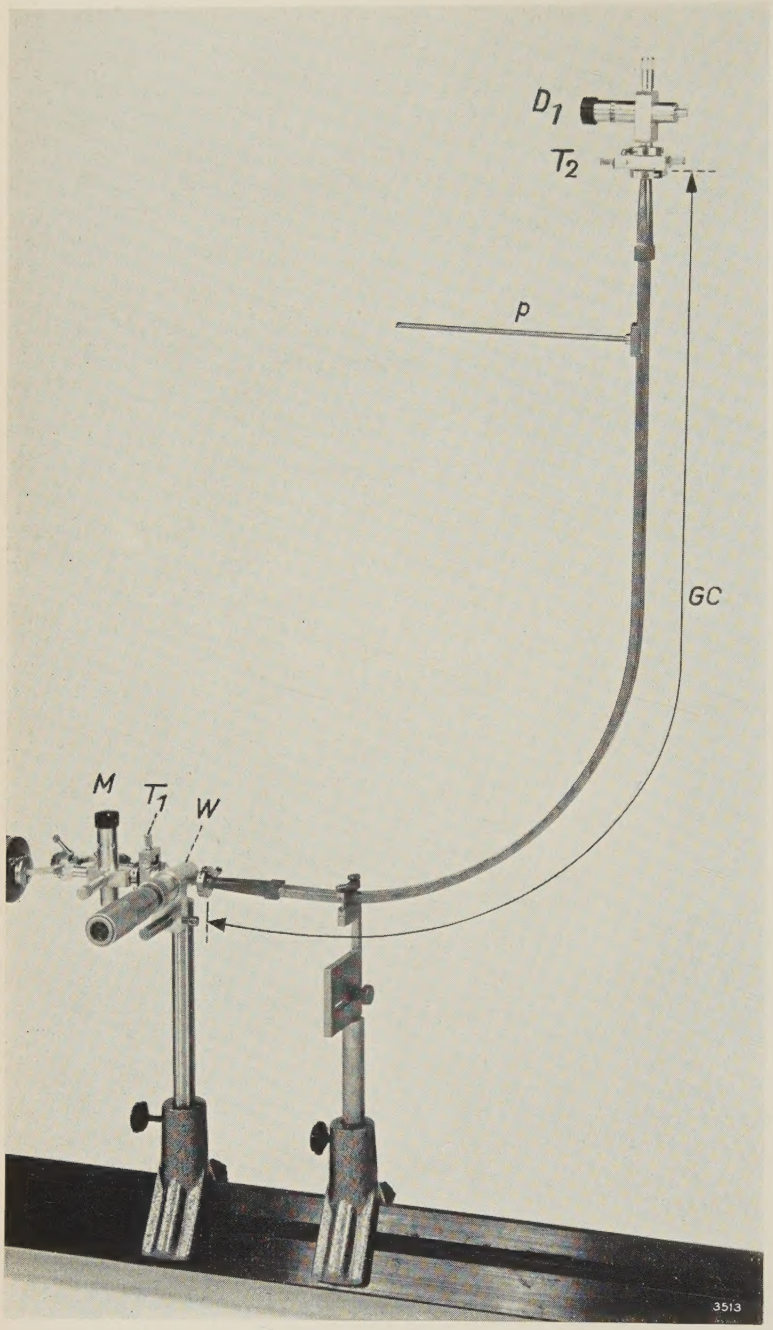

Fig. 10. The 2 mm part of the set-up, the diagram of which is reproduced in fig. 9. p is the pump connection to the gas cell GC (8 mm waveguide). Notation otherwise as in fig. 9. For the purpose of monitoring a wavemeter (W) (TE_{01n} mode) is included in the 2 mm part.

cell is made gas-tight by providing the transitions with mica windows (c and d in fig. 9). In fig. 10 the pump connection p is visible, this being used to evacuate the gas cell before the admission of the gas sample.

One gas that exhibits an absorption line in the neighbourhood of 2 mm wavelength is carbonyl sulphide (COS). The COS molecule is a linear rotator, i.e. the three constituent atoms lie on a straight line (S = C = O), and the molecule rotates about an axis perpendicular to this line. The transitions between the rotational levels lie within the microwave region. Thus, for COS, the following transitions in the 2 mm region have been calculated:

transition from level 9 to level 10 at 121.625 Gc/s,
transition from level 11 to level 12 at 145.947 Gc/s,
transition from level 13 to level 14 at 170.267 Gc/s.

The method of measuring these absorption frequencies will now be described [7]). For this purpose, we choose the line in the neighbourhood of 146 Gc/s. The repeller voltage of the klystron is modulated by the sawtooth voltage which is used for the time-base of the oscilloscope O. The klystron oscillates only when the instantaneous value v_r of the repeller voltage lies between the limits V_{r1} and V_{r2}, and in this region the frequency f varies more or less linearly with v_r (*fig. 11*). In this way, a certain frequency region

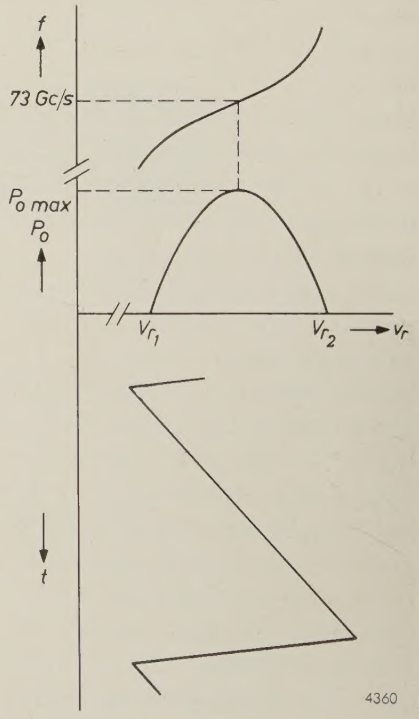

Fig. 11. The repeller voltage v_r of the klystron in fig. 9 has a sawtooth waveform. The klystron oscillates between the limits V_{r1} and V_{r2}. The output power P_o and frequency f vary as shown. At $P_o = P_{o\,max}$ the value of f must be approximately 73 Gc/s.

[7]) C. G. Montgomery, Technique of microwave measurements, M.I.T. Radiation Lab. Ser., Vol. 11, McGraw-Hill, New York 1947, p. 24-33.

is covered [8]). The frequency sweep has a value of, for example, 0.1 Gc/s and the sweep must take place about the value 73 Gc/s approximately; this frequency must occur in the neighbourhood of the maximum output power $P_{o\,max}$.

A check on whether the latter conditions are fulfilled can be made by switching off the generator G and connecting the oscilloscope to the frequency multiplier M, which now acts temporarily as a 4 mm detector. This will give an oscillogram of the type shown in *fig. 12*, which represents the power characteristic of the klystron — P_o as a function of v_r (and therefore of f) — with a superimposed dip caused by the absorption in the 4 mm wavemeter. The latter is tuned to 73 Gc/s. If the klystron is properly tuned, then the peak of the curve occurs at the same frequency as the dip. If this is not so, then the klystron must be mechanically adjusted until the maximum *does* coincide with the dip.

Using the circuit of fig. 9, when *no* gas is present in the cell, an oscillogram of the type shown in *fig. 13a* is obtained. When the cell contains COS gas, the picture obtained is as shown in fig. 13*b*, where the absorption line is visible. The sharper this line is, the more accurately the frequency can be determined. At a given cell volume, the line width increases as the gas pressure rises; this is the result of the interaction between the molecules. An excessive microwave power has a similar detrimental effect because of the saturation which then occurs at the higher level.

The determination of the frequency is achieved in the first instance with the aid of a 4 mm or 2 mm wavemeter. With, for example, a carefully calibrated

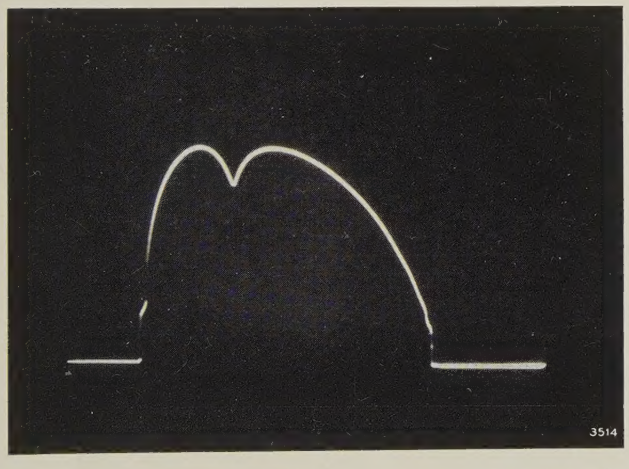

Fig. 12. Oscillogram of the detected output power P_o from the klystron; the abscissa represents both time and frequency. The dip marks the frequency to which the wavemeter is tuned (73 Gc/s), the klystron being mechanically adjusted so that the peak of P_o occurs at this frequency.

[8]) Use is thus made of the "electronic tuning range" of the reflex klystron; see Philips tech. Rev. **21**, 224 (fig. 6, Note [4])), 1959/60 (No. 8).

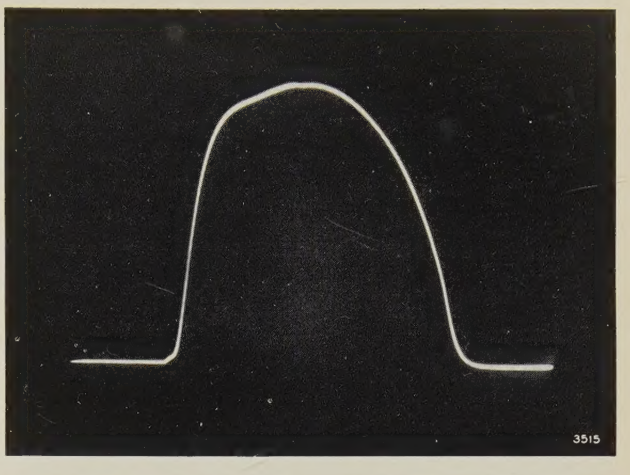

a

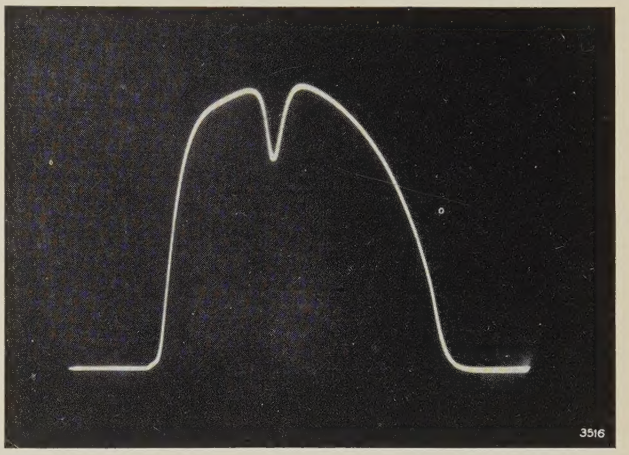

b

Fig. 13. Oscillograms obtained from the oscilloscope O of fig. 9, *a*) evacuated gas cell, *b*) gas cell filled with COS gas. The absorption line in (*b*) occurs at a frequency of approximately 146 Gc/s.

TE_{01n} wavemeter of good construction, the measurement can be made with an accuracy of up to 0.01%. For greater accuracy, more elaborate equipment is necessary [9]), including a frequency standard which is regularly checked. However, the discussion of this does not fall within the scope of this article.

[9]) O. R. Gilliam, Ch. M. Johnson and W. Gordy, Microwave spectroscopy in the region from two to three millimeters, Phys. Rev. **78**, 140-144, 1950.

Summary. In continuation of Part I of this article, in which waveguide components for 2 mm wavelength were discussed, Part II describes three measuring set-ups. The first of these is for measuring dissipative losses of the order of 0.1 to 3 dB in microwave components. In the second set-up, the reflection coefficients of unknown impedances are determined by means of a bridge circuit using a hybrid T. With certain precautions, voltage reflection coefficients lower than 0.01 can be measured with reasonable accuracy. The third set-up is used for the experimental determination of absorption lines in gases. The gas carbonyl sulphide (COS), which exhibits an absorption line at about 146 Gc/s, is chosen as an example. Some 2 mm components are also discussed which were not treated in Part I: a crystal detector, a waveguide switch and an isolator.

SOLID-STATE RESEARCH AT LOW TEMPERATURES

I. INTRODUCTION

576.48

by J. VOLGER.

In the first decade of this century, the last "permanent gas", helium, was liquefied by Kamerlingh Onnes in the physics laboratory at Leiden University. Even at that time, however, interest was not confined exclusively to the thermodynamic properties of gases difficult to liquefy; investigations were already being made into the properties of solids in the new temperature range opened up. It was in the course of low-temperature research on the electrical conductivity of pure metals, for example, that superconductivity was discovered. Kamerlingh Onnes — whose name the laboratory now bears — rendered a valuable service to science in that he opened up the field of very-low-temperature research by devising equipment for the routine liquefaction of helium and other not readily condensable gases. Laboratory facilities of this kind were then virtually unique in the world.

Since then, solid-state research has expanded enormously and investigations at low temperatures are made into the most diverse properties. The author has chosen a number of instances of the work being done in this field, at the Philips laboratories and elsewhere, which will be presented in the form of three articles. It will be the aim in each subject discussed to explain why it is so important that the properties in question should be studied at low temperature.

The first article printed below, which is by way of an introduction to the subject, begins by considering what exactly is meant by "low temperature".

In recent decades, cooling to extremely low temperatures has become a valuable research tool. The properties of solids, for instance — we shall not be concerned with liquids and gases in these articles — often exhibit characteristic changes at low temperature, from which inferences may be drawn regarding the structure of the substances investigated. Structure in this sense refers not merely to the geometry of the crystal lattice, whether or not perturbed by lattice defects, but also, for example, to the spectrum of possible lattice vibrations and the location and structure of the bands of energy levels occupied by electrons.

In this series of articles we shall endeavour to illustrate with a number of examples the scientific importance of low-temperature research, and also, where relevant, its technological importance. First, however, it will be useful to consider what is meant by "low" temperature. We shall see that the answer differs from case to case, and that in some instances even room temperature may be regarded as very low. Our considerations will be confined, however, to those properties of solids which show characteristic changes only after cooling to temperatures lower than about 50 °K.

The concept "low temperature"

The criterion as to whether a temperature is to be regarded as "low" is to be found in the phenomenon in which we are interested. We may, for example, take the transition from the liquid to the solid phase, a phenomenon shown in principle by all substances at a sufficiently low temperature (with the exception of helium if the pressure is too low). It is found that in substances of corresponding crystal structure the melting point T_S — which we regard in this case as the upper limit of the region where the temperature may be called low — is approximately proportional to the heat of fusion ΔU. In *Table I* it is seen that $\Delta U/T_S$ is indeed roughly constant for the simple substances chosen, even though the values of ΔU and T_S themselves differ considerably.

Table I. Comparison of the heat of fusion ΔU per gram-molecule and the melting point T_S of various substances. For substances of simple crystal structure the ratios $\Delta U/T_S$ have much about the same value. In the case of water (ice), whose structure is more complicated, the value of $\Delta U/T_S$ differs considerably from that of the simpler structures.

Substance	H_2	N_2	Ar	Ag	H_2O
Heat of fusion (J/mole)	126	960	1170	11300	6040
Melting point (°K)	16	63	84	1230	273
Ratio $\Delta U/T_S$	8.0	15.0	13.8	9.2	22

The provisional conclusion, then, is that the limit of what we may regard as the low-temperature region is determined by an energy that is characteristic of the phenomenon involved.

A description of the solidification or fusion process by the methods of thermodynamics involves, apart from energy and temperature, the concepts of order and disorder. The degree of disorder may be expressed thermodynamically in terms of the entropy S; a high value of S corresponds to a greater degree of disorder.

In the fusion of a solid under constant pressure the heat supplied is not used for raising the temperature but solely for bringing about the fusion, i.e. for creating a state of greater disorder. According to thermodynamics the process of fusion involves no change in the *free enthalpy* G — also known as the Gibbs free energy or the thermodynamic potential — which is defined by the equation $G = U - TS + pV$ (where U is the internal energy, T the absolute temperature, S the entropy, p the pressure and V the volume). The transition is therefore given by:

$$\Delta U - T_S \Delta S + p\Delta V = 0\,, \quad . \quad . \quad . \quad . \quad \text{(I.1)}$$

or, since, for a liquid-solid transition, $p\Delta V$ may be neglected:

$$\Delta S \approx \frac{\Delta U}{T_S}. \quad . \quad . \quad . \quad . \quad . \quad . \quad . \quad . \quad \text{(I.2)}$$

The entropy change (per mole) upon fusion is thus equal to the heat of fusion divided by the melting point.

Substances of corresponding crystal structure may be expected to have roughly the same value of ΔS, and hence a similar value of $\Delta U/T_S$. (In the gas-to-liquid transitions the spread in the values of ΔS is even smaller than in the solidification process. This finds expression in Trouton's rule.)

Looking at the situation now more from the *molecular* point of view, it should be noted first of all that temperature is a quantity we use to describe merely the *macroscopic* state of the substance; the temperature concept is not applicable to individual molecules. The relation between the temperature of a system — we shall see later that a "system" does not necessarily imply a "quantity of matter" — and the energy of the individual molecules, is given by *statistical mechanics*. Although we cannot possibly do justice to the principles of statistical mechanics [1]) within the scope of this article, we shall nevertheless try to show their significance for the subject under consideration. To do this we take the following example.

The specific heat of a quantized system

Suppose that a substance consists of molecules whose energy can have only the values E_1, E_2, ... E_n, ... and which exhibit no marked interaction, so that the total energy of the substance is specified almost entirely by the sum of the energy contributions of each of the molecules. Now statistical mechanics tells us that, when such a system is in thermal equilibrium, the probability $W(E_n)$ that a molecule will have the energy E_n is given by the formula:

$$W(E_n) = g_n \exp\,(-E_n/kT). \quad . \quad . \quad . \quad \text{(I.3)}$$

In this expression, k is Boltzmann's constant (1.38×10^{-23} J °K^{-1}), T the absolute temperature, and g_n the degeneracy of the energy level of rank n.

An energy level has a degeneracy of, say, 3 if it corresponds to three distinct quantum states of the molecule (atom) all having the same energy. The degeneracy can be removed by an external perturbing influence, e.g. by the application of a strong electric or magnetic field. The energies of the three states are then generally altered by unequal amounts, so that the threefold degenerate level breaks up into three non-degenerate levels. The splitting-up of the spectrum lines of a gas discharge subjected to a magnetic field (Zeeman effect) is an example of this.

From (I.3) we can immediately derive an expression for the average energy $\bar{E}$ of the molecules:

$$E = \frac{\Sigma\, E_n g_n \exp\,(-E_n/kT)}{\Sigma\, g_n \exp\,(-E_n/kT)}. \quad . \quad . \quad \text{(I.4)}$$

On the assumption that each molecule of our substance may be treated as a (quantized) harmonic oscillator, the quantum theory states that the values which the energy may assume are equal to $\frac{1}{2}h\nu$, $1\frac{1}{2}h\nu$, $2\frac{1}{2}h\nu$, ... $(n - \frac{1}{2})h\nu$, ..., where h is Planck's constant (6.6×10^{-34} J sec), ν the frequency of the oscillator, and n is again the rank number. Substituting this in (I.4) we find, after some manipulation [2]), the Planck-Einstein formula:

$$\bar{E} = \tfrac{1}{2}h\nu + \frac{h\nu}{\exp\,(h\nu/kT) - 1}. \quad . \quad . \quad \text{(I.5)}$$

If the temperature is so high that $kT \gg h\nu$, we may write as a fair approximation:

$$\bar{E} = kT. \quad . \quad . \quad . \quad . \quad . \quad . \quad . \quad \text{(I.6)}$$

In this temperature range, then, the energy of the system is proportional to T. Its specific heat, which is equal to $N\,\mathrm{d}\bar{E}/\mathrm{d}T$, is therefore constant, viz. Nk per gram-molecule, where N is Avogadro's number. This is no longer true when the system is cooled down to temperatures where kT becomes of the same order of magnitude as $h\nu$. At temperatures where $kT \ll h\nu$, the average energy of the molecules

[1]) An introduction to statistical mechanics is given by J. D. Fast, Entropy in science and technology, Philips tech. Rev. **16**, 258-269, 298-308 and 321-332, 1954/55. A more advanced treatment will be found in:
R. C. Tolman, Statistical mechanics with applications to physics and chemistry, New York 1927;
D. ter Haar, Elements of statistical mechanics, New York 1954;
L. D. Landau and E. M. Lifschitz, Statistical physics, London 1958, to name only a few.

[2]) See e.g. C. Kittel, Solid state physics, 2nd impression, p. 123, Wiley, New York 1957.

is given by

$$E \approx \tfrac{1}{2}h\nu + h\nu \exp(-h\nu/kT). \quad . \quad . \quad . \quad (I.7)$$

The specific heat C is now no longer constant but depends on T. The variation of E and C with temperature is shown in *fig. 1*.

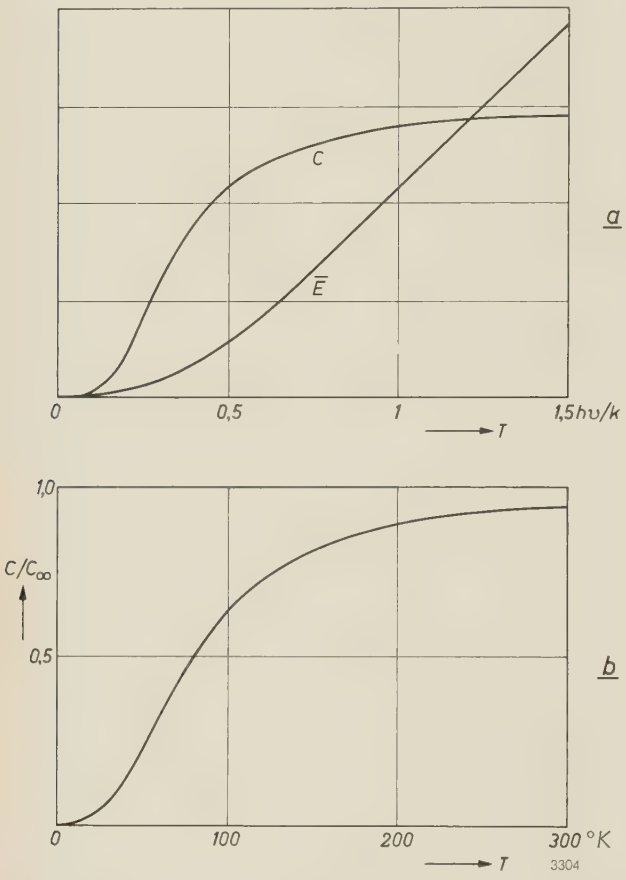

Fig. 1. *a*) The theoretical variation with temperature T of the average molecular energy $\bar{E}$ and the specific heat C of a solid, when the molecules are treated as non-interacting quantized harmonic oscillators. When $kT \gg h\nu$, the energy E increases linearly with T, and the specific heat is constant. The low-temperature region is the region where kT is of the order of magnitude of $h\nu$, or smaller. *b*) Variation of the specific heat of copper with temperature (after Debye [3]).

Fig. 1*a* is a plot of $\bar{E}$ according to (I.7) and the specific-heat curve derived from it; fig. 1*b* illustrates how the specific heat of copper varies as a function of temperature. In spite of the sweeping simplifications in our example, the two curves show a remarkable resemblance.

We see that, according to statistical mechanics, the temperature in the above example may be qualified as "low" in the region where kT is smaller than the energy $h\nu$. *As a general rule, low-temperature physics is concerned with the temperature region where kT is smaller than a certain characteristic molecular (or atomic) energy.*

[3]) P. Debye, Ann. Physik **39**, 789, 1912.

Reverting to the example of the liquid-to-solid transition, we note that there the ratio $\Delta U/T_S$, calculated per mole, was approximately equal to Nk ($Nk = 8.32$ J/mole °K). Although in itself a macroscopic quantity, the heat of fusion may also be regarded in a sense as a molecular quantity, since its value depends closely on the energy with which a molecule (atom, ion) is bound to its site in the crystal lattice.

Finally, it should be pointed out that the quantity kT, which constantly occurs in statistical mechanics, does not always emerge from a distribution function of the type (I.3). The latter (due to Boltzmann) applies only to particles which obey the laws of "classical" statistics. The free electrons in a metal, for example, which collectively form a kind of "gas" about 10^4 times as dense as an ordinary gas at normal temperature and pressure, and whose mass is roughly 10^4 times smaller than that of ordinary gas molecules, are described by the Fermi-Dirac distribution function; to the "gas" of light quanta (photons) in a closed space the Bose-Einstein distribution function applies.

The existence of various different distribution functions is due to differences in the methods of calculating the number of states in which the system may be found. In the classical theory this is done on the underlying assumption that each molecule of a gas is distinguishable and in principle could be followed on its way. In quantum statistics identical particles are regarded as indistinguishable, and moreover states which can be derived from each other simply by the exchange of two identical particles are treated as the same state (one might thus say that the particles are not only indistinguishable but have no individuality). This change leads to the Bose-Einstein distribution. Where particles are concerned to which the Pauli exclusion principle applies — "no two particles can be in exactly the same quantum state" — (e.g. electrons), we come to the Fermi-Dirac distribution. Both quantum distributions reduce to the Boltzmann relation in the case of "gases" which are so rarefied that the distance between the particles is large compared with their De Broglie wavelength.

Paramagnetism

As a third example of the general rule that the low-temperature region can be found by comparing kT with a certain energy, we shall consider *paramagnetism*. By contrast with the two preceding examples, which served purely for illustration, the considerations here may serve as an introduction to the section on paramagnetic phenomena, which will appear in the third article of this series.

It will be known that paramagnetism arises from the fact that the electrons which together form the electron cloud of an atom, or ion, possess a magnetic (spin and orbital) moment. In many substances the electron clouds of the ions that make up the crystal lattice have what is called the "inert-gas structure", and the total moment is zero. There are

some ions, however — e.g. those of the iron group — whose electron shells are not completely filled, and these do show a resultant moment. When a paramagnetic substance is placed in a magnetic field H, the component of the magnetic moment in the direction of H can only assume certain discrete values, and the energy-level diagram shows correspondingly discrete levels. Generally, the distance between these levels is primarily determined by the strength of the applied field and further by the interaction of the magnetic atoms with neighbouring atoms (which may or may not be magnetic).

In the simplest case the magnetic moment can take up only two positions, with components of magnitude μ_B parallel or antiparallel to H (μ_B being the Bohr magneton). The energy difference between the two levels is then $2\mu_B H$. Here again, the occupation of the levels follows from the Boltzmann equation (I.3), and by a method similar to that used for deriving (I.4) we find that the average magnetic moment $\bar{\mu}$ is given by:

$$\bar{\mu} = \mu_B \frac{\exp(\mu_B H/kT) - \exp(-\mu_B H/kT)}{\exp(\mu_B H/kT) + \exp(-\mu_B H/kT)} = \mu_B \tanh \frac{\mu_B H}{kT}. \quad . \quad . \quad (I.8)$$

For $kT \gg \mu_B H$, this yields the Langevin-Curie formula for the susceptibility χ, the ratio between the resultant moment $\bar{\mu}N$ of a gram-atom and the magnetic field H:

$$\chi = N\mu_B{}^2/kT. \quad . \quad . \quad . \quad . \quad (I.9)$$

The results obtained with less simple energy-level diagrams are not essentially different from the above, provided kT is again greater than the energy range in which the levels are situated.

The variation of $\bar{\mu}$ with T, as expressed in (I.8), is plotted in *fig. 2*. The transition between the region of high temperature, where $\bar{\mu}$ is small and proportional to H, and the region of low temperature, where saturation occurs, is seen to lie between 1 and 2 °K for an applied magnetic field of 10^6 A/m (12 500 oersteds). Virtually complete saturation occurs only below 1 °K. The fact that the upper limit of the low-temperature region must be very low in this case may be directly inferred from (I.8), bearing in mind that $N\mu_B H$ at 10^6 A/m is equal to only 7.0 J/mole, and that NkT at $T = 1$ °K is as much as 8.3 J/mole.

Free electrons in metals and semiconductors

As an introduction to the second article of this series, we shall now touch on some aspects of electrical conduction in metals and semiconductors.

It is common knowledge that, in most metals, every atom loses a certain number of electrons (usually one), and these electrons seem to move as free particles through the lattice; theoretically they may be regarded as independent. The energy levels they may occupy are so close together as to form effectively a continuous band. Broadly speaking, this band of energy levels is filled only up to a certain "height". As mentioned earlier, the occupation of energy levels in an "electron gas" is given not by the Boltzmann distribution but by application of Fermi-Dirac statistics. The occupation $f(E)dE$ of a narrow strip dE of the energy band in which the density of the quantum states [4]) has the value $g(E)$ is given by:

$$f(E)dE = \frac{g(E)dE}{1 + \exp(E - E_F)/kT}. \quad . \quad (I.10)$$

In this expression E_F is the energy of the Fermi level, which may be regarded to a first approximation as independent of temperature. We may deduce from this formula that, at absolute zero, $f(E) = g(E)$ for particles of energy $E \leqq E_F$, and $f(E) = 0$ for energies $E > E_F$. This means that all levels are filled below the Fermi level ($E \leqq E_F$) — with only *one* particle in each quantum state, in accordance with the Pauli exclusion principle — and all other levels are empty. Since the value of E_F for metals amounts to one or two electronvolts, and the value of kT at room temperature is only about $\frac{1}{40}$ eV, a metal at room temperature is already to be regarded as very cold. Although some levels for which $E > E_F$ are in fact occupied at this

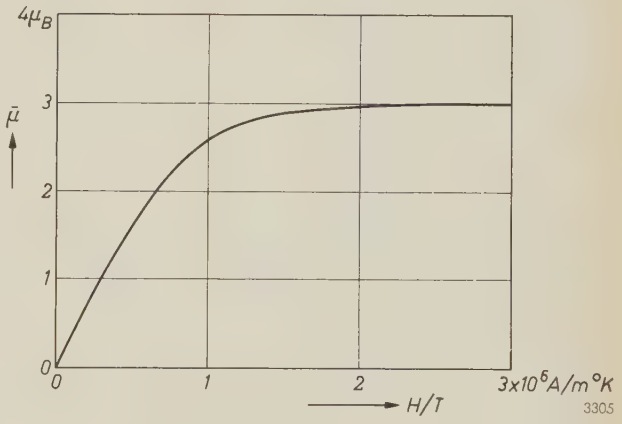

Fig. 2. The magnetization $\bar{\mu}$ of a paramagnetic substance is proportional to H/T at high temperature (Langevin-Curie law), and virtually constant (saturation) even in weak fields at low temperature. For an applied field of 10^6 A/m (12 500 oersteds), the transition region lies between 1 and 2 °K.

[4]) If there is no degeneracy at all, the density of the quantum states is equal to the density of the energy levels.

temperature, the occupation is nevertheless equal in good approximation to that obtaining at $T = 0$ (degenerate electron gas; see *fig. 3*). The reasons underlying the anomalous behaviour of the electrical conductivity of metals below 50 °K are therefore usually of an entirely different nature. That their study can contribute to our knowledge of the solid state will be explained later in these articles.

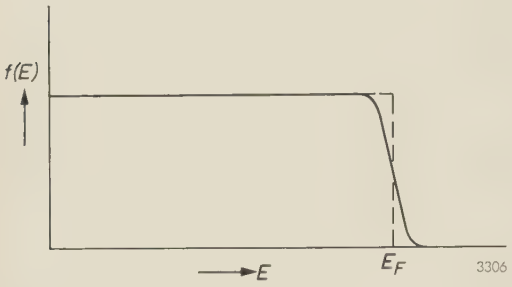

Fig. 3. In a metal the occupation f(E) of the energy levels by conduction electrons is such that virtually all levels below the Fermi energy E_F are filled and those above it empty. At room temperature (solid line) the occupation differs slightly from that which would exist at absolute zero (dashed line), by an amount of the order of kT ($\approx \frac{1}{40}$ eV at room temperature). The value of E_F is a few electron volts (1 eV $\approx k \times 10^4$ °K).

As may be inferred from the foregoing, the value of E_F can be found directly by integrating formula (I.10) and equating $\int f(E)dE$ with the total number of electrons. The form of the function f(E) will of course depend on the properties of the crystal lattice concerned, and will therefore differ from case to case. In the case of metals the value assumed by E_F at absolute zero (E_F is not, as we have seen, entirely independent of temperature) is found to be:

$$E_{F_0} = 4.2 \times 10^{-11} \times (m/m^*) n_0^{\frac{3}{2}} \text{ eV}. \quad . \; . \quad \text{(I.11)}$$

Here n_0 is the concentration of the free electrons, m the mass of the electron and m^* its effective mass in the relevant lattice. The effective mass m^* has the significance that the motion of an electron acted upon by external forces can be described as if the electron were a particle of mass m^* moving in free space instead of through a crystal lattice.

One last remark. We have said that, because a metal is effectively very cold at room temperature, any anomalous effects it may show below that temperature are not connected with the occupation of the energy levels. Sometimes, however, this may not be entirely true, particularly if g(E) has anomalous values at E values close to E_F, as it has in sodium, for example.

In semiconductors the situation as a rule is quite different. Bands of energy levels are separated here by forbidden bands, i.e. zones of energy in which there are no levels at all. At low temperature there is very often an entirely filled band (valence band) and well above it an entirely empty one (conduction band). Only at a relatively high temperature can an electron acquire sufficient energy to reach the conduction band. In semiconductors the number of free electrons is therefore very much smaller than in metals. Frequently — in the case of "extrinsic semiconductors" — the free electrons are not supplied by the atoms or molecules of the substance itself but by foreign atoms (donor impurities); the concentration of the free electrons is then a function of the impurity concentration too. These electrons are released from the donor atoms by thermal agitation, at the cost of an ionization energy ΔE.

At temperatures where $kT \ll \Delta E$, virtually all electrons will evidently be bound to the donors, and from the above considerations we should then expect these impure substances to be insulators, just as chemically pure semiconductors are at a sufficiently low temperature. However, even in this temperature range, conduction does take place in some of these substances, apparently in consequence of a different mechanism.

The idea underlying this "impurity band conduction" is that the electrons do not first have to be excited sufficiently to promote them directly into a level in the conduction band, but that they "jump" from one donor to another. Of course, between the region of high temperature, where normal conduction via the conduction band dominates, and the region of very low temperature, where impurity band conduction prevails, there is a transitional region where both mechanisms make a substantial contribution to the current. The effects observed in this region will be discussed in the second article of this series.

It may be useful to comment here briefly on an aspect of the behaviour of free electrons in semiconductors, which was not mentioned above because its consequences will not be discussed in these articles. As we have seen, the free electrons in a metal are described by the Fermi-Dirac statistics; a metal, statistically speaking, is always "very cold". This is not so in the case of semiconductors. It is possible in some semiconductors to control the nature of the impurity concentration in such a way that, in the temperature range of the experiments, the Maxwell-Boltzmann statistics apply at high temperatures and the Fermi-Dirac statistics at low temperatures. In the region of transition between the two statistics, particularly interesting effects are found. For most impurity semiconductors the Boltzmann distribution usually applies, and therefore their conductivity is much more temperature-dependent than that of metals.

In conclusion it should be mentioned that very many solid-state processes, such as the orientation of the ions (electron spins) in a paramagnetic salt subjected to a magnetic field, take place through the intermediary of lattice vibrations. When the

temperature falls, these vibrations become weaker, thereby slowing down the processes concerned. If we regard the lattice vibrations as the vibrations of quantized oscillators, then the ratio of kT to the magnitude of the energy quanta is the determining factor. This aspect of the low-temperature behaviour of solids will also be discussed in one of the following articles in this series.

Summary. This introductory article, the first of three on solid-state research at low temperatures, shows by a number of examples that a system may be said to be at a low temperature when kT is smaller than a certain characteristic energy. This is the energy quantum $h\nu$ for the specific heat of a system of quantized harmonic oscillators, the heat of fusion (per mole) for the fusion of a solid, the energy $\mu_B H$ for the magnetization of a paramagnetic substance, and the Fermi energy E_F for the electrical conductivity of metals and semiconductors. The article concludes with the remark that many solid-state processes, e.g. the orientation of electron spins in a paramagnetic substance, are slowed down at low temperature.

AN OMEGATRON FOR THE QUANTITATIVE ANALYSIS OF GASES

by A. KLOPFER *) and W. SCHMIDT *).

621.384.8:621.039.343

The present tendency towards high vacua of lower and lower pressures both in laboratory equipment and in electron tubes and other industrial products, makes it important to determine accurately the composition as well as the total pressure of the residual gas. Among the various kinds of mass spectrometer used for this purpose, the omegatron is particularly well suited — as this article describes — for determining, qualitatively and quantitatively, the composition of a gas at pressures lower than 10^{-5} mm Hg.

For some years past, omegatrons have been developed and used in various laboratories for determining the composition of residual gases in high-vacuum systems. The first description of an omegatron was given by Sommer, Thomas and Hipple in 1951 [1]). The usefulness of the instrument was demonstrated by Alpert and Buritz in 1954 with a simplified arrangement [2]), which quickly found application in many laboratories.

The omegatron has been used at Philips since 1953 for *qualitative* analysis of the residual gas in sealed-off cathode-ray tubes [3]). With a view to making the instrument suitable for *quantitative* analyses, investigations were undertaken which have led to the omegatron described in this article.

Principle of the omegatron

The operation of the omegatron was described in this journal some years ago. We shall briefly recapitulate here the underlying principle. A perspective sketch of the instrument is shown in *fig. 1*. A narrow beam of electrons from a cathode K runs parallel to a uniform magnetic field B. Electrons colliding with gas molecules give rise to ions. If the latter have a velocity component perpendicular to the direction of the magnetic field, they describe circular paths perpendicular to the (static) magnetic field. The radii of these paths are given by the equation:

$$r = \frac{m}{e}\frac{v_0}{B}, \quad \ldots\ldots \quad (1)$$

where m is the mass of the ion, e its charge, v_0 the velocity component perpendicular to the direction of the magnetic field and B the field-strength (or

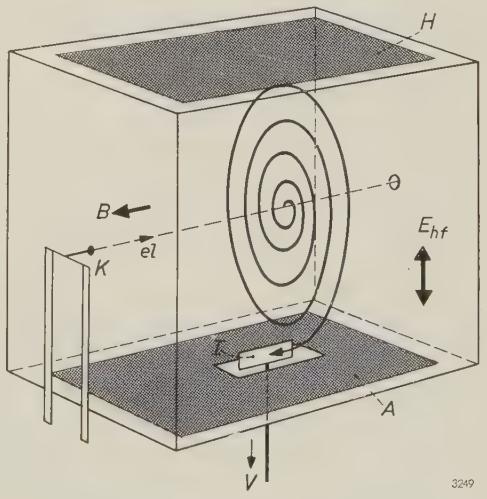

Fig. 1. Perspective sketch of a simplified omegatron. B indicates the direction of the magnetic induction, E_{hf} the direction of the RF field. The figure illustrates the spiral path described by an ion. K cathode, which emits the ionizing beam of electrons *el*. A and H are the electrodes to which the RF voltage is applied. I ion collector. V connection to amplifier.

*) Philips Zentrallaboratorium GmbH, Aachen Laboratory.

1) H. Sommer, H. A. Thomas and J. A. Hipple, Phys. Rev. **82**, 697, 1951.
2) D. Alpert and R. S. Buritz, J. appl. Phys. **25**, 202, 1954.
3) J. Peper, Philips tech. Rev. **19**, 218, 1957/58.

rather the magnetic induction, using the rationalized Giorgi system). The angular frequency ω_c of the revolution of the ion is:

$$\omega_c = \frac{e}{m} B, \quad \ldots\ldots \quad (2)$$

and the period of revolution is therefore independent of the velocity v_0. This is the same situation as in a cyclotron, and just as in that case an RF field $\hat{E}_{hf} \sin \omega t$ is now applied perpendicular to the magnetic field. The effect of this is that the orbiting ions are accelerated or slowed down, depending on the value of e/m (i.e. their angular frequency) and their phase. If we make the frequency ω of the alternating electric field equal to the angular frequency ω_c of a given kind of ion, the result is a condition of resonance. An ion in the correct phase then absorbs an equal quantity of energy upon each revolution, and thus describes a spiral of uniformly increasing radius (equiangular or Archimedes spiral). The resonating ions can be caught on a suitably placed collector electrode, and the ion current detected with the aid of a sensitive amplifier.

Ions having some other mass or charge (i.e. a different angular frequency) and which are thus not in resonance, also describe spiral paths, that is to say orbits whose radius varies with time. However, the maximum value of this radius generally remains smaller than the distance between the point of origin of the ions and the collector, and therefore such ions do not contribute to the measured current.

In order to determine the composition of a gas mixture, the frequency of the electric field applied to the omegatron must be varied either continuously or in steps. When a collector current, due to ions in resonance, is measured at a particular frequency, the e/m ratio of these ions can be found from equation (2). It is then possible to determine the kind of gas concerned. The collisions between electrons and gas molecules give rise not only to singly ionized gas molecules, but also to doubly or multiply ionized particles. The gas molecules may also be broken up into ionized or neutral particles. In this way one finds for any type of gas and any given electron energy a complete "ionic spectrum", having a series of peaks corresponding to the respective masses of the particles, and with constant ratios between the heights of the peaks. For any gas these ratios, which correspond to the relative ion current measured at the respective resonant frequencies, can now be found by calibration; see *Table I*. When the omegatron contains an unknown gas, its nature can be deduced from the measured intensities for the various mass numbers by comparing the ratios between the ascertained values with the ionic spectra determined by calibration.

The pressure of each component of the gas mixture can in principle be found from the ion current, provided the relation between the pressure and the ion current is reproducible. With an electron current i^- and a pressure p, the ion current i_0^+ is given by:

$$i_0^+ = s \sigma p i^-, \quad \ldots\ldots \quad (3)$$

where s in the effective length of the electron beam through the gas, and σ is the probability of ionization. But not all the resonant ions produced reach the ion collector. Some of them are lost by collision with gas molecules. Of the ions that do not collide with gas molecules, a fraction α reaches the

Table I. Relative heights of the peaks due to ions of various masses for a number of gases (the peak of the most commonly occurring mass of each gas is taken as 100). In most cases the true mass of the gas will be that corresponding to the highest peak; see e.g. H_2O. This is not always so, however; see for example C_3H_8.

Gas \ Mass	2	12	13	14	15	16	17	18	19	20	24	25
H_2	100	—	—	—	—	—	—	—	—	—	—	—
Ar	—	—	—	—	—	—	—			14.2	—	—
H_2O	0.6-1.5	—	—	—	—	1.8	21	100	11-17	0.23	—	—
N_2	—	—	—	7.4	0.03	—	—	—	—	—	—	—
CO	—	3.3	0.04	0.55	—	1.3	—	—	—	—	—	—
CO_2	—	3.5	0.03	0.08	—	7.8	—	—	—	—	—	—
CH_4		1.8	5.7	12.5	81	100	2.7	—	—	—	—	—
C_2H_2	3.5	1.4	4.0	0.3	0.04	—	—	—	—	—	5.1	19
C_2H_4		0.6	1.0	2.3	0.3	0.4	—	—	—	—	2.0	6.8
C_2H_6		0.2	0.55	2.0	3.1	0.15	—	—	—	—	0.5	2.7
C_3H_8		0.18	0.36	1.13	3.8	0.12	—	—	—	—	0.13	0.64

collector, and the remaining part (1—α) arrives on the other electrodes. The current i^+ incident on the ion collector is therefore:

$$i^+ = \alpha\, i_0{}^+ \, e^{-L/\lambda} = \alpha\, s\, \sigma\, p\, i^- \, e^{-L/\lambda}, \quad . \; . \; . \quad (4)$$

where L represents the total path length of the resonating ions and λ the mean free path. In most cases, λ will be very much greater than L. The requirement that the relation between i^+ and p should be reproducible amounts to saying that, for given values of the parameters s, σ, L and λ and a given electron current i^-, the coefficient α should be constant. It is particularly important that α should not depend on the state of the instrument, nor on the presence of other gases whose ions are not in resonance. The ideal, of course, would be $\alpha = 1$. Let us consider the effects that can make α smaller than unity and upset the reproducibility.

As a result of their thermal energy, the ions have a tendency to escape from the plane of their spiral path, i.e. in the direction of the magnetic field. A weak electrostatic field is therefore applied which hinders this tendency. There are then in the middle of the omegatron components of the electric field which are perpendicular to the magnetic field. The effect of this is that the ions can describe cycloidal paths along the equipotentials. We shall return to this problem later. As a result of charged layers on the electrodes, the electrostatic field in the tube may undergo unpredictable variations, and thus affect the probability of ions escaping. Ions that are not in resonance may give rise to space-charge effects, which are dependent on the pressure and also influence the equipotential surfaces of the electrostatic field. Because of all these effects, α is not constant with time and moreover differs from one tube to another. Since the fields produced by the effects referred to are of the same order of magnitude as the applied electrostatic field, widely divergent values may be found for α (between 0 and 1). These variations of α made it impossible to use the omegatron in its original form for quantitative analyses.

Omegatron with side plates

In the Philips Aachen Laboratory an omegatron has now been developed whose sensitivity can be adjusted to give a constant value of $\alpha = 1$, the sensitivity being the ion current divided by the product of electron current and pressure. The tube is shown schematically in *fig. 2*. The left half of the figure represents a cross-section parallel to the direction of the magnetic field. In this section the omegatron has its original form [1]). The cathode K emits electrons which are accelerated through the omegatron parallel to the magnetic field and are finally caught by the electron collector T. To minimize the reactions of the gas with the hot cathode, a cathode is used which can operate at a relatively low temperature, namely a directly heated barium-oxide cathode [4]). The electrode G_1 may be used for stabilizing the electron current. The electrode G_2 has roughly the same electrical potential as the electron collector T. The omegatron must be aligned with extreme accuracy between the poles of the magnet, in order to prevent electrons striking the electrode A. This can be checked with a microammeter. If the alignment is not accurate, the secondary electrons formed will affect the space charge and hence the sensitivity. The RF voltage

[4]) The use of this cathode was suggested by J. Peper. For various reactions of gases with cathodes, see the article by S. Garbe in Advances in vacuum science and technology, Proc. first int. Congress Vac. Tech., Namur 1958, Vol. I, p. 404, Pergamon Press, Oxford 1960.

28	29	30	31	32	36	37	38	39	40	41	43	44	Mass / Gas
—	—	—	—	—	—	—	—	—	—	—	—	—	H_2
—	—	—	—	—	0.38	—	0.06	—	100	—	—	—	Ar
—	—	—	—	0.13	—	—	—	—	—	—	—	—	H_2O
100	0.75	—	—	—	—	—	—	—	—	—	—	—	N_2
100	0.88	0.2	—	0.02	—	—	—	—	—	—	—	—	CO
11.5	0.1	—	—	0.4	—	—	—	—	—	—	—	100	CO_2
—	1 - 5	—	—	—	—	—	—	—	—	—	—	—	CH_4
—	—	—	—	—	—	—	—	—	—	—	—	—	C_2H_2
100	3.3	—	—	—	—	—	—	—	—	—	—	—	C_2H_4
100	20.5	25.9	0.54	—	—	—	—	—	—	—	—	—	C_2H_6
60.3	100	2.1	—	—	0.64	4.1	5.8	20	—	16	30.8	44.9	C_3H_8

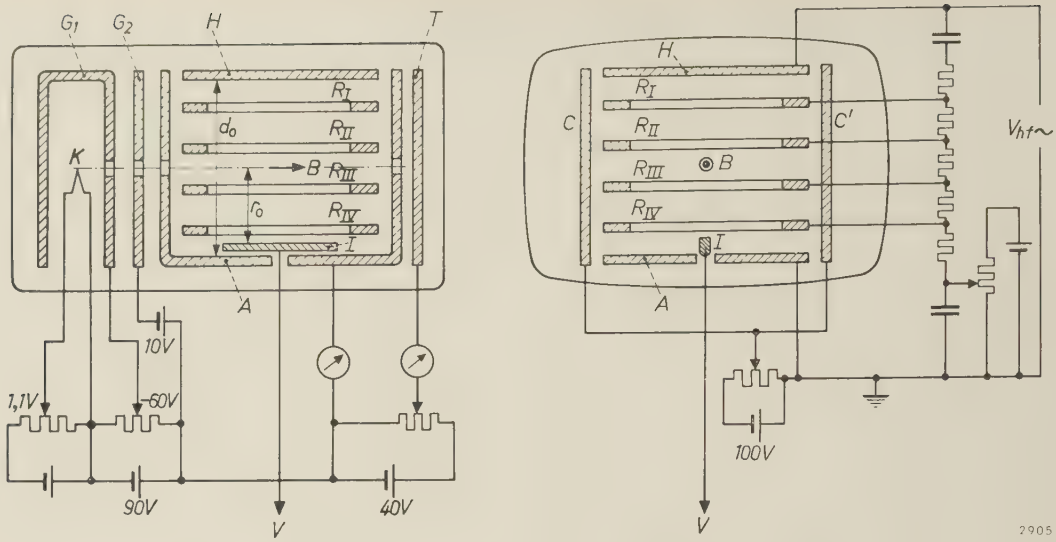

Fig. 2. Schematic representation of omegatron with rings R_I-R_{IV} and side plates C-C'. The left part of the figure shows the section parallel to the magnetic field, the right half a section perpendicular to the magnetic field (induction B). K-G_1-G_2 electron gun. T electron collector. I ion collector. The RF voltage is applied between the electrodes A and H. Other potentials are applied to the electrodes as indicated in the figure. The amplifier is connected at V.

is applied between the electrodes A and H. The flat parallel rings R are all held at a small positive electrostatic voltage; this serves to prevent the escape of ions in the direction of the magnetic field. In addition, RF voltage is applied to the rings R, a different amplitude for each ring (obtained by means of a voltage divider); this measure helps to establish a uniform RF field.

The right half of fig. 2 shows the cross-section perpendicular to the magnetic field. The main difference compared with the original form is the addition of two side plates C and C'. By giving these plates a negative potential with respect to the electrodes A and H, a suitable electrostatic field is created in the omegatron, that helps to make the sensitivity of the tube reproducible. We shall deal with this in more detail presently. The magnitude of this potential, required to obtain a maximum ion current on the ion collector, depends on the positive static potential V_R on the rings R, as well as on their number. It is found that, when four rings are used, a value of approximately 1 : 100 is a suitable choice for the ratio $V_R : V_{CC'}$.

The arrangement is made clearer by the sketch of the cut-away electrode system shown in *fig. 3*. The photograph in *fig. 4* gives an idea of the dimensions of the omegatron in its glass envelope. The electrodes form a cube having edges 25 mm in length. Using no ceramic or mica, they are mounted on a glass foot and surrounded by a glass envelope. The whole tube can be degassed in an oven at 400 °C. The electrodes separately may be degassed at 900 °C by high-frequency heating. This high temperature sometimes proves to be necessary in order to remove disturbing surface layers on the electrodes. If the omegatron is not to be baked out in this way, the choice of electrode material is not critical, provided the electrodes have been thoroughly cleaned beforehand. A heat treatment is always desirable, however, in order to minimize the release of gases from glass and metal surfaces. To prevent the formation of oxide layers during the degassing process, considerable use is made of noble metals. The best results

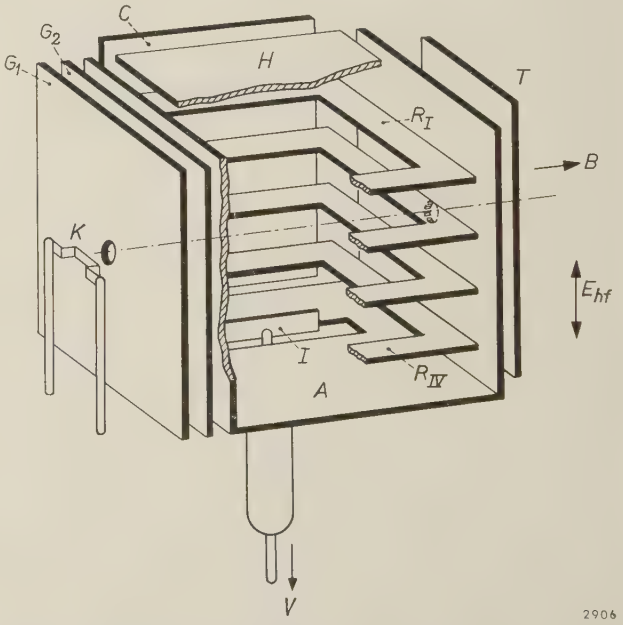

Fig. 3. Cut-away view of omegatron, showing rings and side plates (still somewhat schematic). Notation as in fig. 2.

were obtained with an alloy of platinum and iridium.

Little need be said about the auxiliary apparatus used with the omegatron. A permanent magnet or an electromagnet is used for producing the magnetic

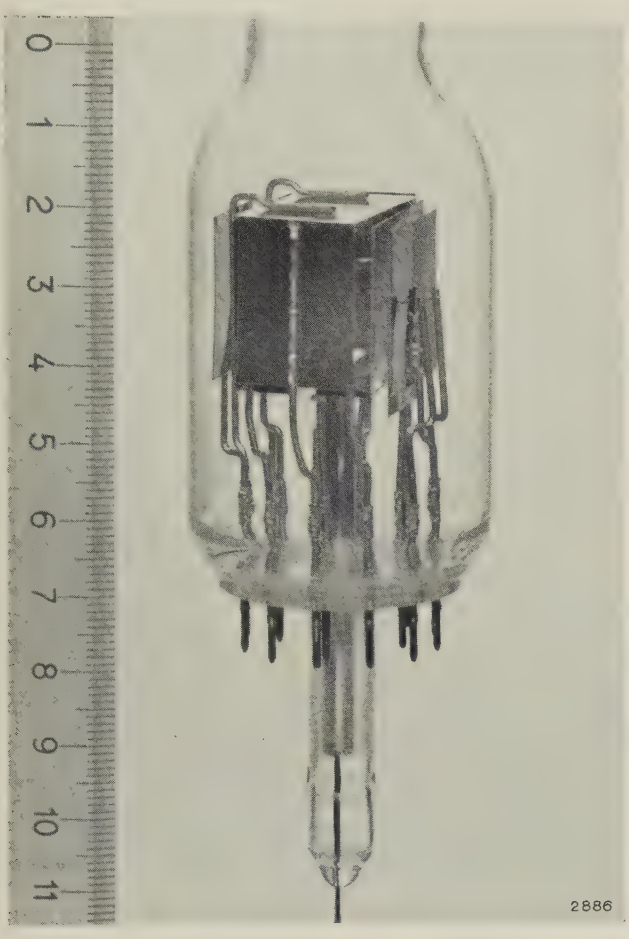

Fig. 4. The omegatron, with rings and side plates, in a glass envelope. The cathode is on the right, and on the extreme left is the collector for the electrons which have traversed the omegatron. The ions formed in the space inside the omegatron move to the ion collector. This is connected to the central metal pin fused into the glass tube.

field. The permissible non-uniformity of the magnetic field over the omegatron is 2%. Any commercial signal generator may be used as the voltage source for the RF field, provided the output amounts to a few volts and is independent of frequency.

The lowest measurable pressure of a given type of gas is determined by the lowest measurable direct current. A vibrating-reed electrometer is therefore particularly suitable for this measurement. Since the smallest currents which this can measure are of the order of 10^{-16} ampere, the connection between the ion collector and the electrometer input should be well screened.

Stabilization of the electron current proved to be essential. For this purpose a fixed potential is applied to the electrode G_1 and a resistance incorporated in the cathode lead. The electron current is then stabilized, via the space charge, by the voltage drop across the cathode resistor.

The mass spectrogram can be recorded on an oscilloscope or with a recording instrument as earlier described [3]).

Operation of the omegatron with side plates

Consider the imaginary plane through the middle of the omegatron perpendicular to the magnetic field. The electrostatic equipotential lines in that plane are represented in *fig. 5*, where the rings are omitted for the sake of simplicity. The magnetic field is perpendicular to the plane of the drawing. The electrodes C and C' have a negative static potential of a few tens of volts with respect to A and H. At this stage we shall disregard the effects of the RF field and the space charge in the omegatron. Electrolytic-tank measurements [5]) of the electrical field in the omegatron showed that at all points in the plane under consideration there exists a small negative potential, between a few tenths and one volt, in relation to the electrodes A, H and I, except in the edge regions around the rings R. Depending on where they are formed, positive ions now pass along the equipotential lines in cycloidal paths outwards. The directions are indicated in the figure. To avoid ions escaping in the direction pointing away from the ion collector, the position P where the ions are formed should lie on the ion-collector side of the electrical centre-point M as shown in fig. 5. The

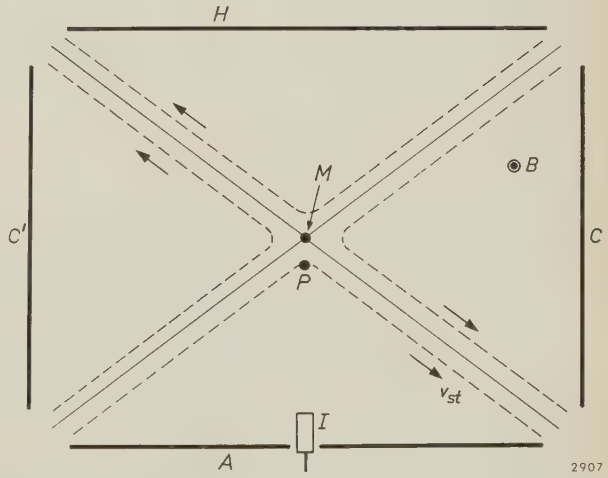

Fig. 5. Cross-section of omegatron perpendicular to the direction of the magnetic field. M is the electrical centre, P the position where the ions are formed. I ion collector. A and H electrodes to which the RF voltage is applied. C and C' side plates, which are given a negative potential with respect to A and H. The dashed lines represent equipotential lines.

[5]) These measurements were done by J. L. Verster and L. G. J. ter Haar at Eindhoven.

mere presence of the ion collector electrode I contributes to the required asymmetry. The precise position required of P with respect to M (as in fig. 5) is obtained by careful choice of the position of the electrode H.

When a high-frequency alternating electric field is now applied, a spiral path is superposed on the cycloidal path already described by the ion. The resultant motion can be regarded as one in which the ions describe spiral paths whose centre moves continually outwards at a velocity v_{st}. The result will be that the ions which are not in resonance are drawn outwards. This will have the effect of reducing the space charge. The ions which *are* in resonance describe a path that will make for an optimum ion capture at the ion collector. These highly intricate ionic movements lead to complicated considerations on the influence of the various parameters to be chosen. We shall try to deal with these considerations quite briefly.

To achieve optimum ion collection we must stipulate certain conditions regarding the magnitude of the electrostatic and RF fields. The velocity v_{st} is proportional to the electrostatic field-strength E_{st} and inversely proportional [6]) to the induction B:

$$v_{st} \propto \frac{E_{st}}{B}. \quad \ldots\ldots \quad (5)$$

The value E_{st} should be chosen large enough to ensure that the potential is not seriously affected by the space charge. An upper limit is set to E_{st}, however, by the amplitude of the RF field. This may be understood as follows. The rate at which the radius of the spiral paths of the resonating ions increases is proportional to the RF field [1]):

$$v_{hf} \propto \frac{E_{hf}}{B}. \quad \ldots\ldots \quad (6)$$

If E_{st} is taken too large, and the RF field E_{hf} is too small, an ion in resonance is unable, in the time available, to acquire sufficient energy to reach the ion collector. If we raise E_{hf} we admittedly increase the energy which the ion can take up per revolution, but we adversely affect the resolution ($m/\Delta m$). Consequently the region within which E_{st} may be chosen is somewhat limited.

Whilst the upper limit of the amplitude of the RF field E_{hf} is determined by the resolution, the lower limit of E_{hf} depends on the ion acquiring in the available time sufficient energy to reach the ion collector at the minimum value of E_{st}. Otherwise the ion will not reach the collector and will be lost by collision with other electrodes.

Finally, it should be noted that v_{st} and v_{hf} are approximately independent of the mass of the ions. The values selected for maximizing the ion current at a given gas pressure are therefore valid for the whole mass spectrum of arbitrary gas mixtures.

When the ion capture is optimum, α in equation (4) may be put equal to 1. The fact that this is permissible is to be seen from *Table II*. Here the values σ for the probability of ionization, as reported in the literature, are compared with the values of σ that may be calculated from our experiments on the assumption that $\alpha = 1$. We proceed as follows. The ion current is measured at a known pressure and a given electron current. With the aid of equation (4) the value of σ can then be determined, provided the effective length s of the electron beam and the total length L of the orbit of the resonating ions are known. The length s is a constant and equal to 1.1 cm in the omegatron described. The length L is a function of the pressure p, the induction B, the RF field E_{hf}, the mass m of the ion in resonance and the dimensions of the omegatron. The value of L so derived is inserted in equation (4), yielding:

$$i^+ = \alpha i^- p s \sigma \exp\left[-\frac{2.7\times10^{-5} r_0^2 d_0}{\lambda_0 p_0} \frac{B^2 p}{V_{hf} m} \right], \quad (7)$$

where $\lambda_0 p_0$ is the pressure-independent product of the mean free path and pressure [7])[8]), p is the pressure of the only type of gas assumed to be present in the omegatron, and V_{hf} is the r.m.s. RF voltage; the meaning of r_0 and d_0 is explained in fig. 2.

The values of σ found from (7) correspond to the values reported in the literature if $\alpha = 1$. In other words, all resonating ions that do not collide with

Table II. Values of the ionization probability σ for various kinds of gas determined with the omegatron compared with values given in the literature. The unit is the number of ion pairs per electron and per centimetre path length, at a pressure of 1 mm Hg.

Gas	Mass	σ_{exp}	σ_{lit}
H_2	2	3.6	3.6
He	4	1.63	1.36
N_2	28	10	10
CO	28	10.7	10
Ar	40	11.8	12

[6]) L. Spitzer jr., Physics of fully ionized gases, Interscience Publishers, New York 1956.

[7]) R. Jaeckel, Kleinste Drucke, ihre Messung und Erzeugung, Springer, Berlin 1950.

[8]) S. Dushman, Scientific foundations of vacuum technique, Wiley, New York 1949.

gas molecules are captured by the collector. *Fig. 6* shows the result for helium. From Table II it may be seen that the correspondence is even better for other gases.

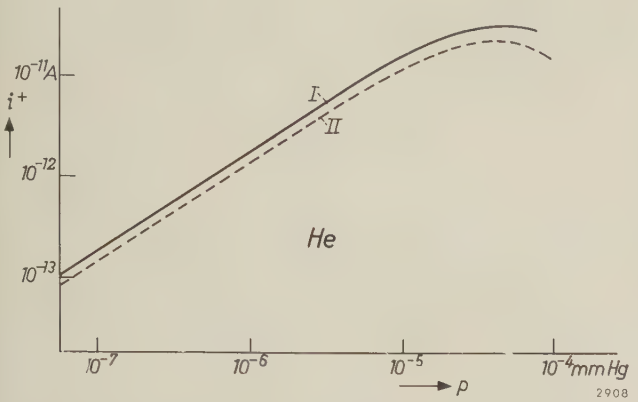

Fig. 6. The ion current i^+ as a function of pressure p, the omegatron containing helium only. Curve *I* gives the experimental values, curve *II* the theoretical values.

Choice of parameters

Having shown in the foregoing that the omegatron can be used for quantitative analyses, we shall now discuss in more detail the choice of various parameters which affect the properties of the omegatron.

1) The *electrostatic field-strength* in the omegatron must be adjusted by the small positive potential V_R and the negative potential $V_{CC'}$ on plates C and C' in such a way that the current of the ions in resonance will be maximum at a given pressure. The setting of these values is critical, since an ion current may flow even when no RF field has been applied. This residual current, as it is called, is proportional to the total pressure, i.e. the sum of the pressures of all gas components. It is attributable to the strong space charge that may be produced when there are low negative potentials on the side plates C and C'. The potential at the point of origin of the ions can then be equal to the potential of the ion collector. The residual currents measured in such a case are represented by the dashed curves in *figs. 7* and *8*. The solid curves represent the relation between the ion current and $V_{CC'}$ (fig. 7) and V_R (fig. 8), when the amplitude of the RF voltage is 1 V_{rms} and the magnetic induction 0.5 Wb/m². For the values of V_R or $V_{CC'}$ where a residual current arises in the absence of an RF field, ions that are not in resonance will still reach the collector even when this field is present. Consequently it is possible that the ratio i^+/i^+_{max} in the solid curves of fig. 8 will exceed the value of 1. To avoid interference from residual currents, it is best to choose a small positive

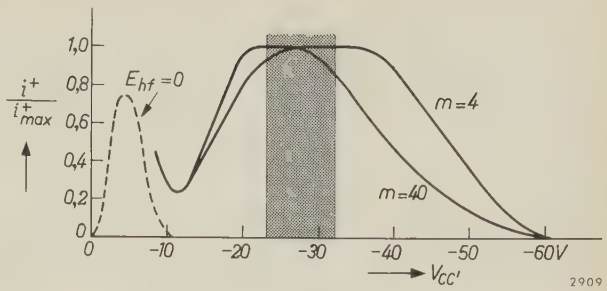

Fig. 7. Illustrating the effect which the negative potential $V_{CC'}$ (on the side plates C and C') has on the ion current i^+. V_R = 0.15 V; V_{hf} = 1 V_{rms}; i^- = 1 μA; B = 0.5 Wb/m². The solid curves represent the relative ion current for the mass numbers 4 and 40. The dashed curve represents the ion current reaching the collector in the absence of an RF field (residual current). The shaded area is the operating region.

voltage V_R and large negative voltages $V_{CC'}$ (see the shaded regions in figs. 7 and 8). Owing to absorbed surface layers on the electrodes, the optimum values may vary from one tube to another.

2) According to equations (4) and (7) the ion current at a given pressure is independent of the *RF voltage* V_{hf} when $\lambda \gg L$. If this condition is no longer satisfied, the ion current decreases, and it does so more rapidly for light than for heavy particles. In the omegatron described, the ion current decreases faster than might be deduced from equation (7). This is due to the fact that, with electrostatic fields present in the omegatron, the resonance frequencies are a function of position. There is then a minimum value of the RF voltage at which the ions in resonance are still only just capable of reaching the ion collector [9]). Since the ion loss when the RF voltage is too low differs for each kind of ion, it is always necessary to operate the omegatron in the "saturation region"; in other words, the ion current must be independent of the RF voltage. Only then will the

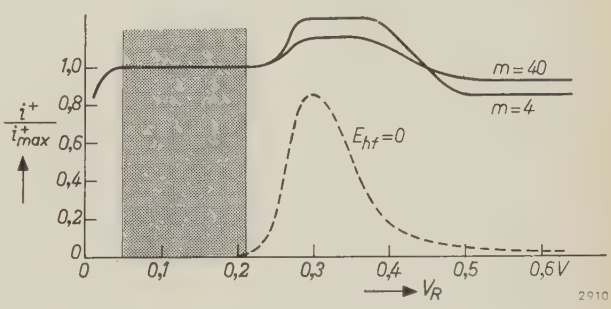

Fig. 8. Curves showing how the ion current i^+ depends on the positive potential V_R on the rings R. $V_{CC'}$ = — 25 V; V_{hf} = 1 V_{rms}; i^- = 1 μA; B = 0.5 Wb/m². The dashed curve represents the ion current reaching the collector in the absence of an RF field. The shaded area is the operating region.

---

[9]) W. M. Brubaker and G. D. Perkins, Rev. sci. Instr. **27**, 720, 1956.

pressures of the various components of the gas mixture be measured in their correct relationships. Generally the RF voltage will be roughly 1 V_{rms}.

3) The *voltage V_T of the electron collector* has little influence on the ion current provided this electrode is clean.

4) According to equation (4) the ion current at a given pressure is a linear function of the *electron current*. If the electron current is too high, the large numbers of ions formed will give rise to a strong space charge, which affects the electrostatic field. The ion current will then no longer be a linear function of the electron current. *Table III* shows for various pressure ranges the maximum permissible electron currents at which, irrespective of the mass, the relation between ion current and electron current is still linear.

Table III. The permissible electron current i^- for various levels of the total pressure p. The higher the total pressure, the smaller the permissible electron current.

p mm Hg	i^- μA
$\leqq 10^{-8}$	30
$\leqq 10^{-7}$	10
$\leqq 10^{-5}$	1

Pressure range, resolution and accuracy of measurement

From (7) the maximum permissible pressure is calculated to be 10^{-5} mm Hg where the induction B is 0.5 Wb/m² and the amplitude of the RF voltage V_{hf} corresponds to 1 V_{rms}. At this pressure the mean free path λ is still $\gg L$, irrespective of the gas composition. At lower pressures than 10^{-5} mm Hg the relation between ion current and electron current is then linear provided the electron current is not greater than 1 μA (see Table III).

The lowest pressure p_{min} measurable with the omegatron is determined by the smallest ion current which the electrometer is capable of measuring at the maximum permissible electron current:

$$p_{min} = \frac{i^+_{min}}{s\sigma i^-_{max}} \quad . \quad . \quad . \quad . \quad . \quad (8)$$

Inserting $i^+_{min} = 10^{-16}$ A, $i^-_{max} = 3\times10^{-5}$ A, $s = 1.1$ cm and $\sigma = 10$, we find $p_{min} = 3\times10^{-13}$ mm Hg. The lowest pressure measured in our laboratory was approximately $p_{min} = 1\times10^{-12}$ mm Hg. As mentioned above, some gases can only be identified from their ion spectrum. If relative intensities of 1 : 100 are found between the ions (or agglomerates) of the various mass numbers, the lowest pressure that can be measured for any one type of gas is $p_{min} \approx 3\times10^{-11}$ mm Hg.

The resolution [1]) of the ideal omegatron, i.e. one in which the electrostatic field and the thermal energy of the ions in the direction of the magnetic field are zero, is given by the expression:

$$\frac{m}{\Delta m} = \frac{eS_0B^2}{2\hat{E}_{hf}m} \quad . \quad . \quad . \quad . \quad . \quad . \quad (9)$$

This formula is arrived at on the assumption that, in the spectrogram, the peaks for the masses m and $m \pm \Delta m$ are separated right down to the base. In the present instance, S_0 is the distance from the ion collector to the point on the equipotential line where the centre of the spiral path lies after the total time of flight of the resonant ion. In the ideal omegatron, $S_0 = r_0$. For an induction $B = 0.5$ Wb/m² and an RF field corresponding to $V_{hf} = 1$ V_{rms}, a resolution can usually be achieved such that at a mass number of 30 one mass number can still be resolved. In the ideal omegatron, according to equation (9), this would be possible up to the mass number 39. It is possible to increase the resolution by increasing the magnetic field. Reducing the RF voltage increases the resolution only very slightly, since this voltage may only be varied within the saturation region.

The sensitivity of the tube described remains constant up to 10% provided the electrode surfaces are clean. If the geometry of the various tubes is identical, so is their sensitivity. About 40 of these omegatrons were tested in our laboratory on their reproducibility. The presence of gases and vapours such as H_2O, CH_4, C_2H_6 and CO_2 up to maximum pressures of 10^{-5} mm Hg caused no change in the sensitivity, even after several weeks on test. However, the presence of Hg and also HCl on the electrodes causes marked changes in sensitivity. The accuracy with which the pressure of a pure gas can be determined amounts to 10%. In the case of a gas mixture, the error may be much greater, particularly if different components of the gas mixture contribute to the same mass peak (see Table I). All gases that contribute less than 10% to the ion current at this mass remain undetected.

The omegatron of the type described has been used at Philips for a variety of investigations, including the analysis of residual gases in vacuum equipment and in electron tubes, the investigation of reactions between getter and gas, and the determination of the release of gases from various kinds of glass.

Fig. 9 shows a simple example of a mass spectrogram obtained in an investigation of the residual gases in a well-outgassed glass system containing a barium getter film.

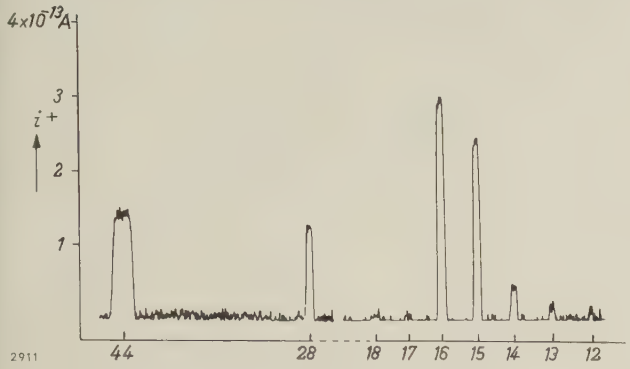

Fig. 9. Mass spectrogram of the residual gas in a vacuum system in which a barium getter has been flashed. The composition of the gas (expressed in partial pressures) is as follows.

CH_4:	2.8×10^{-9} mm Hg	N_2 :	2×10^{-10} mm Hg
CO_2:	1.0×10^{-9} mm Hg	C_2H_6:	2×10^{-10} mm Hg
CO :	8×10^{-10} mm Hg	H_2O:	1×10^{-10} mm Hg

Summary. In the manufacture of electron tubes and other industrial products, and also for high-vacuum work in laboratories, it is important to know not only the total pressure but also the composition of the residual gas. For this purpose, use is often made of the omegatron. In its original form, this instrument provided only qualitative results. This article describes a type of omegatron which can also be used for quantitative analyses. To make this possible a pair of side plates have been added to the original instrument. When a suitable potential is applied to these plates, the ion current can be brought to an optimum value at any mass which is in resonance.

For a magnetic induction B of 0.5 Wb/m² and an RF voltage of 1 V_{rms}, the maximum permissible pressure is 10^{-5} mm Hg. The lowest measurable pressure of any one kind of gas is $p_{min} \approx 1\times10^{-12}$ mm Hg, when a DC amplifier is available capable of detecting a current of 10^{-16} A. The resolution is such that masses 30 and 31 can be distinguished. The accuracy of measurement is 10%.

METHODS OF PRODUCING STABLE TRANSISTORS

by J. J. A. PLOOS van AMSTEL.

621.794:621.382.3

One of the major problems in the manufacture of transistors is to make them stable, i.e. to produce transistors whose characteristics do not change in the course of time. Such changes are due to surface effects. It is therefore necessary to produce surface conditions that will minimize these changes.

It was originally hoped that the characteristics of junction transistors, by their very nature, would change very little and that, if properly used, the transistors would have an almost unlimited life. Theoretical considerations show that the operation of these transistors is governed by the dimensions and the material properties of the constituent layers, i.e. of the emitter, base and collector [1]), and there is no reason to assume that these dimensions and properties alter in normal operation. At places where the *P-N* junctions reach the surface (see *fig. 1*) there must of course be no surface layer that might give rise to an undesired conductive path between the *P* and *N* regions. In the fabrication of transistors, cleaning the surface by etching is therefore one of the routine operations.

The optimistic expectations regarding the stability of transistors have not been borne out, however. It very soon appeared that, in spite of the etching, the state of the germanium surface has a very pronounced influence on the properties of the transistor. The electrical changes observed are very often due to changes in this surface — as, for example, the adsorption of foreign molecules and atoms — and these in their turn are bound up with the state of the ambient atmosphere. The obvious way to seek improvement was therefore to hermetically encapsulate the transistors. This, however, proved to be insufficient: life tests showed that the parameters — in particular the current amplification factor — continued to change. The production of stable transistors was more difficult than was at first thought.

In many laboratories the surface of germanium, and semiconductor surface phenomena in general, have consequently been the subject of much experimental and theoretical research [2]). One of the aims pursued was to find methods of achieving surface conditions that would result in good transistors and moreover ensure a high degree of stability. This article will describe some results of investigations

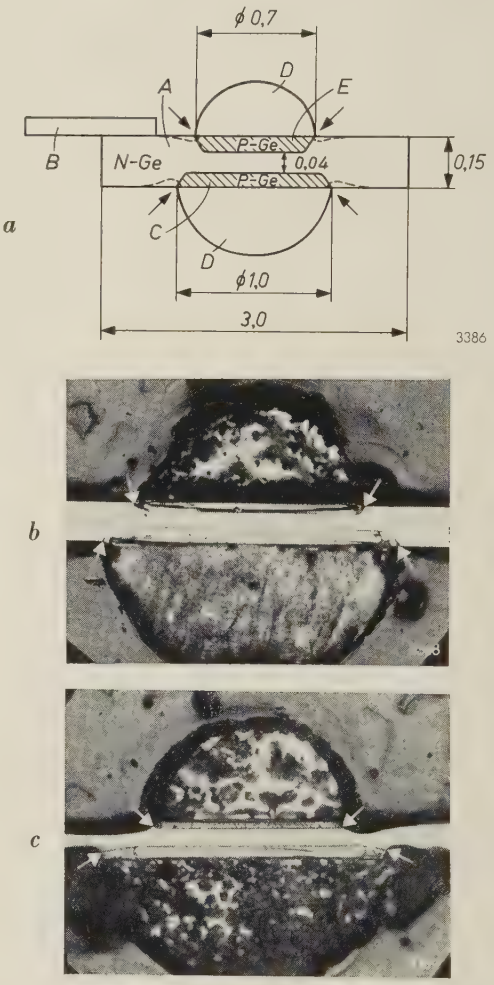

Fig. 1. *a*) Schematic cross-section of a *P-N-P* junction transistor, made by the alloying method. Dimensions in millimetres. *A* germanium single crystal of type *N* in the form of a wafer ($3 \times 2 \times 0.15$ mm). *B* base contact. *C* collector; this part of the germanium crystal is given *P*-type conductivity by alloying with the acceptor material *D*. *E* emitter, also of *P*-type germanium due to alloying with *D*. The arrows indicate where the *P-N* junctions reach the surface. After etching, the surface follows the dashed lines.
b) Polished cross-section, on which the various regions are made visible by etching. The arrows again indicate the *P-N* junctions at the surface. The transistor is here surrounded by a layer of shellac in connection with the preparation of the sample.
c) As *b*), but with etched surface.

[1]) See F. H. Stieltjes and L. J. Tummers, Simple theory of the junction transistor, Philips tech. Rev. **17**, 233-246, 1955/56, and F. H. Stieltjes and L. J. Tummers, Behaviour of the transistor at high current densities, Philips tech. Rev. **18**, 61-68, 1956/57.

[2]) R. H. Kingston, Review of germanium surface phenomena, J. appl. Phys. **27**, 101-114, 1956.

undertaken along these lines at Philips Research Laboratories at Eindhoven. The investigations concerned *N-P-N* and *P-N-P* germanium transistors for low frequencies and low power, made by the alloying method. A schematic cross-section of this type of transistor *(P-N-P)* is shown in fig. 1, together with the relevant dimensions.

The marked influence which the surface has on the operation of a transistor is accounted for by assuming that holes and electrons recombine at the surface to an extent that depends strongly on the state of the surface. To explain this effect, let us consider a *P-N-P* transistor. Here the emitter injects holes into the base, whilst the collector acts as a sink for holes from the base. If no recombination occurs in the base — in a stationary or quasi-stationary state — all injected holes will disappear to the collector, where they contribute to the collector current. That is the ideal situation. In fact, however, holes disappear in the base by recombining with electrons, and are thus lost to the collector current. This "base loss" is one of the two reasons why the ratio of the collector current to the emitter current — called the current amplification factor α — is less than unity [3]). It has been found that the base loss in transistors of the alloy type may largely be due to recombination at the surface. Changes in the velocity of recombination at the surface therefore have a considerable effect on the base loss and hence on the behaviour of the transistor.

We shall look a little closer at the reason for this effect. If we speak of a high surface recombination velocity, we mean that a hole in the neighbourhood of the surface is very likely to be lost by recombination with an electron. Whether there is in fact a high degree of recombination near the surface depends of course on whether there are holes there to be affected. To show that this will certainly be so, we may consider the case where no recombination at all takes place at the surface. *Fig. 2a* roughly illustrates the flow pattern of the hole current in that case, together with the lines of constant hole concentration. The two systems of lines are orthogonal, and the lines of constant concentration must moreover terminate perpendicular to the surface. The hole current must therefore run partly along the surface, so there will indeed be holes there, which may be destroyed by recombination at the surface. The recombination calls for a correction to the pattern in fig. 2*a*. The corrected pattern will look something like that in fig. 2*b*.

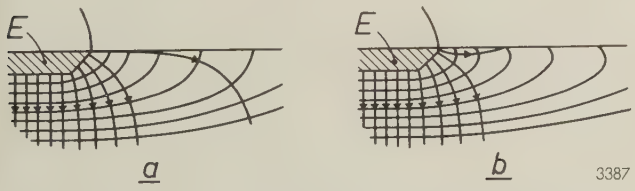

Fig. 2. Illustrating contours of constant hole concentration and the flow lines of the hole current (with arrows) in the base of a *P-N-P* junction transistor at the edge of the emitter *E*. The two sets of lines are orthogonal.
a) The pattern on the assumption that there is no recombination at the surface. The lines of constant hole concentration must then terminate at right-angles to the surface. The hole current passes along the surface; if there is any opportunity for surface recombination, holes will certainly be lost.
b) The pattern after correction for surface recombination. (Recombination inside the base is disregarded in both cases.)

[3]) The second reason is the emitter loss; see p. 239 *et seq.* of the first article quoted in reference [1]).

To make a stable transistor it would be a great help if the surface could be treated in such a way as to make the surface recombination velocity insensitive to extraneous influences. Although work is being done in that direction, the results have so far been unsatisfactory. In this article we shall be solely concerned with the method whereby an attempt is made to reach the same objective by providing the transistor with a suitable *ambient atmosphere*. Obviously, this is possible only if the transistor is enclosed in a hermetically sealed container. We shall see presently why this air-tight enclosure is not in itself enough. There are certain substances that not only reduce the surface recombination velocity to an acceptable value but also, provided they are properly applied inside the enclosure, keep it constant over a long period of operation. Two outstanding representatives of these substances will be discussed here, namely *water* and *arsenic*, particular attention being given to the influence of water, i.e. water vapour.

A sensitive indication of the base loss, and hence of the surface recombination velocity, is the ratio of the collector current to the base current. We denote this "current amplification factor" by α', to distinguish it from the earlier mentioned α, which is the ratio between collector and emitter currents. Between α and α' there exists the well-known relation

$$\alpha' = \frac{\alpha}{1-\alpha},$$

which follows directly from the fact that the sum of the emitter, base and collector currents is zero (provided these currents are counted positive when directed towards the transistor). Since α is not much smaller than unity — at least in a serviceable transistor — α' undergoes greater changes than α. For the purpose of judging the surface effects of the various measures adopted, α' is therefore always measured.

The effect of water

It is known that the surface recombination velocity depends on the surface occupation by water

molecules [4]). When the surface is completely dry, the surface recombination velocity is high, and α' is correspondingly low. As the water "occupation" increases, the surface recombination velocity decreases and α' rises. The changes of α' observed on transistors are therefore certainly to a considerable extent attributable to changes in the water occupation of the surface. Even in hermetically encapsulated transistors, the surface water will almost certainly be affected by temperature variations, for example. The migration of the water may be so slow that one cannot always expect to find the same value of α' at the same temperature. Slow reactions involving water may also play a part.

The most obvious method of eliminating this undesired influence is to make sure that there is no water at all inside the transistor envelope. This is a method that is in fact used, but it has the drawback of resulting in a low value of α'. It appears that the presence of only a minute trace of water is sufficient to make α' unstable.

In the methods discussed in this article an attempt is made to create conditions inside the transistor envelope such as to give the surface of the transistor a water occupation that will ensure a high value of α', and at the same time remain constant with time and temperature.

As we have seen, the surface recombination velocity decreases if the surface water increases. At constant temperature, a state of equilibrium will be reached inside the transistor envelope between the surface water and the water-vapour pressure: the greater the vapour pressure, the more densely will the surface be occupied by water molecules, and hence the greater will be the value of α'. The water-vapour pressure must not, however, be unduly high, for if the surface is too wet, disturbances are caused by superficial ionic currents, one result of which may be the appearance of loops in the current-voltage characteristics of the *P-N* junctions if measured by an AC method. It is known that a high surface water content reduces the sensitivity of the surface recombination velocity to fluctuations of that content [5]). Consequently, we may expect the curve of α' as a function of vapour pressure, the temperature being constant, to gradually flatten out (*fig. 3*). This tendency will be enhanced by the fact that the recombination near the surface gradually loses its importance in relation to the other factors governing α', namely the recombination inside the base and the emitter loss. In general, a favourable surface water occupation is found in air of room temperature with a relative humidity in the region of 60%, the value of α' then being high and little dependent on fluctuations of water-vapour pressure.

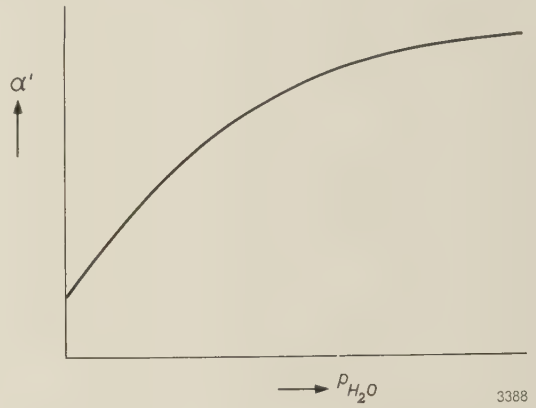

Fig. 3. Expected variation of current amplification factor α' with water-vapour pressure p_{H_2O}, assuming constant temperature and equilibrium between p_{H_2O} and the surface occupation by water.

Stabilization with a water-vapour buffer

It follows from the foregoing considerations that a stable transistor can be obtained by introducing a "stabilizer" inside the encapsulating envelope, i.e. a substance that fixes the water-vapour pressure at a favourable value and thus acts in that respect as a buffer. The stabilizer must ensure a favourable water-vapour pressure at all temperatures which the transistor is likely to reach in normal operation: if the temperature rises, the water-vapour pressure will have to increase in such a way that the existing surface water occupation is maintained. In a graph of temperature t versus water-vapour pressure p_{H_2O} there will be a region of favourable combinations of t and p_{H_2O} as shown by the hatching in *fig. 4*. The water-vapour pressure of the stabilizer as a function of temperature is required to have a curve that lies within this region in the whole temperature interval of interest for the transistor.

Since, in principle, the surface occupation by water is kept constant under all conditions, inertia effects due to changes in surface water no longer occur.

[4]) J. T. Wallmark and R. R. Johnson, Influence of hydration-dehydration of the germanium oxide layer on the characteristics of *P-N-P* transistors, R. C. A. Review **18**, 512-524, 1957; also A. J. Wahl and J. J. Kleimack, Factors affecting reliability of alloy junction transistors, Proc. Inst. Radio Engrs. **44**, 494-502, 1956.

[5]) J. H. Forster and H. S. Veloric, Effect of variations in surface potential on junction characteristics, J. appl. Phys. **30**, 906-914, 1959; also J. R. A. Beale, D. E. Thomas and T. B. Watkins, A method of studying surface barrier height changes on transistors, Proc. Phys. Soc. **72**, 910-914, 1958, and G. Adam, Der Einfluss der Gasatmosphäre auf die Oberflächenrekombination bei Germanium, Z. Naturforschung **12a**, 574-582, 1957.

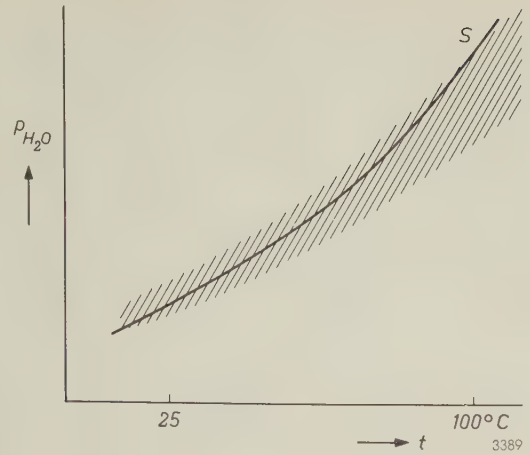

Fig. 4. Illustrating our picture of how the stabilization of transistors with the aid of a water-vapour buffer may occur. The temperature t is plotted versus the water-vapour pressure p_{H_2O} inside the transistor envelope. The hatched region comprises combination of t and p_{H_2O} that produce a favourable occupation of the transistor surface by water. The water-vapour pressure curve S of the stabilizing buffer should lie fully within the hatched region, for the temperature interval of interest.

Stabilization by "forming" the surface

In the following discussion of experiments it will be shown that reasonably stable transistors can be made with the aid of a water-vapour buffer. After prolonged tests, e.g. after some thousands of operating hours, however, α' does usually begin to fall. This drawback can fortunately be overcome by slightly modifying the stabilizing method. A buffer is then used which, at room temperature, gives such a low water-vapour pressure that the surface water remains substantially below the region of favourable values (I in *fig. 5*). A transistor provided with such a buffer therefore has a low α' until it has been subjected to a special treatment. The latter consists of baking the transistor at 140 °C for several days. During the baking process something of the nature of surface "forming" takes place [6]). Our hypothesis is that the region of favourable combinations of temperature and water-vapour pressure for the formed surface is now shifted so as to bring the p_{H_2O} curve for the buffer entirely into the favourable region (fig. 5).

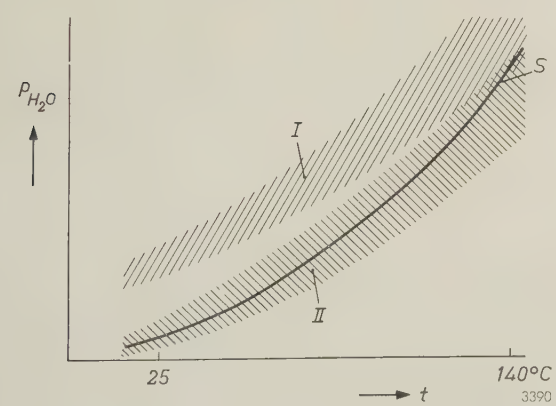

Fig. 5. Schematic representation of a working hypothesis concerning the stabilizing process where the surface of the transistor is "formed" with the aid of a buffer that gives a low water-vapour pressure. t temperature. p_{H_2O} water-vapour pressure. Curve S again represents the vapour pressure of the buffer. Region I covers the combinations of pressure and temperature that correspond to a favourable surface occupation by water *before* forming. After the forming process (prolonged heating at 140 °C) the favourable region corresponds to II.

Experiments

Drying of transistors

With the object of systematically investigating the influence of water vapour on transistors, a drying process was applied during which the change of α' was followed. The transistors were dried both in vacuum and in air. For the vacuum drying the transistors are sealed into a relatively large glass tube (*fig. 6*). The lead-in wires are fused to the glass so far

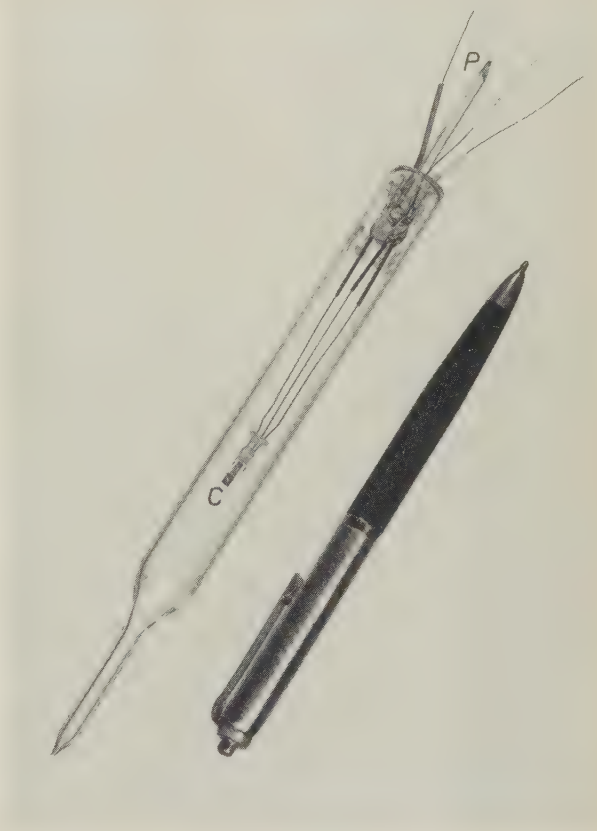

Fig. 6. In the water-vapour experiments the transistors were sealed inside glass tubes so designed that the temperature of the transistors is not significantly affected by the sealing operation. The transistor can be dried under vacuum. P is the pump stem, C the transistor.

[6]) J. T. Wallmark, Influence of surface oxidation on alpha c.b. of germanium P-N-P transistors, R.C.A. Review **18**, 255-271, 1957.

from the transistor that the transistor remains virtually unaffected. When the tube is now evacuated at room temperature, α' gradually falls, but so slowly that the final value is still not reached after days on the pump. Under these conditions the water bound to the germanium is released only very slowly. Evacuation at a higher temperature, e.g. at 100 °C, causes α' to drop faster, but here again, no final value is reached for several days. After pumping at 140 °C, however, α' generally drops in about six hours to a final value which is 10 to 15% of the initial value.

The rate at which α' decreases depends on the pre-treatment of the transistors, particularly on the etching. For example, transistors that have been electrolytically etched in KOH show a much faster drop upon evacuation than transistors that have been etched in acid. However, the final value reached by α' after prolonged pumping at high temperature is always just about as low, whatever the method of etching adopted.

The subsequent admission of a dry atmosphere, e.g. dry air, dry oxygen, or dry nitrogen, has no or scarcely any effect on α' even after long storage. The admission of a humid atmosphere, however, sends α' up again. Sometimes it may rise very rapidly, often increasing in one second by a factor of 5 to 10, sometimes back to its original value. The rate at which α' recovers depends, like the rate at which it falls, on the pre-treatment, that is on the method of etching and on the baking temperature. It depends, too, on the humidity of the air admitted. A relative humidity of 60 % is found to be most effective. After the first steep rise, there is usually a slow increase to the final value.

The fact that the recovery of the transistor is attributable to the water vapour is confirmed by experiments where pure water vapour is admitted to transistors dried in a vacuum. They show that α' recovers in the same way as in humid air. The glass apparatus used for these experiments can be seen in *fig. 7*.

In the drying experiments in air the transistors were heated in a small oven to which air had free access. The behaviour of transistors dried in air is broadly the same as that of transistors dried in vacuum: during the drying process, α' falls at a rate depending on how high the temperature is. Here again, α' falls faster (though not lower) in transistors electrolytically etched in KOH than in acid-etched transistors. Usually the decrease does not continue so far as when the transistors are dried in vacuum, where the drying process is more rigorous. When the dried transistors are again exposed to moist

Fig. 7. Glass apparatus for admitting pure water vapour to vacuum-dried transistors. The marble K is used to break the spherical partition W which seals off the space A containing water. The water-vapour pressure is regulated by the temperature of space A (provided this temperature is lower than that of the space in which the transistor is situated). The apparatus here contains a P-N-P and an N-P-N transistor, for the purpose of comparing the behaviour of the two types.

air, α' again recovers, but normally at a much slower rate than after drying in vacuum. In every case it appears that the state of the surface (i.e. the degree of oxidation) does not affect the rule that a certain surface occupation by water is necessary to obtain a high α', but the surface oxidation does affect certain details of the transistor's behaviour, as for example the rate with which the water makes its presence felt.

To check by other means whether the dehydration of the surface is in fact responsible for the decrease of α', transistors were heated at 140 °C, the water-vapour pressure being increased to maintain a certain surface water occupation. It was found that,

under a water-vapour pressure of 300 to 400 mm Hg, the original values of α' remain virtually unchanged.

Stabilization experiments with a water-vapour buffer

Transistors are frequently sealed into small glass envelopes. It can be seen in *fig. 8* that the dimensions of such an envelope are still considerable compared with the size of the crystal. If this were not so, the crystal would be too near the seal and would be overheated during the sealing operation. Further protection is afforded the crystal by filling the envelope with an appropriate substance. Silicone grease, such as used for high-vacuum purposes, is a suitable and widely used filler.

On page 206 it was argued that stable transistors may be expected if we introduce into the transistor enclosure a buffer which will keep the water-vapour pressure at a favourable value at any working temperature. A silicone grease which has absorbed some moisture, having for example been exposed for 24 hours to air of 30% relative humidity, performs this function reasonably well. *Fig. 9* shows that transistors with a filling of *dry* silicone grease exhibit low values of α' immediately after seal-off, which moreover drop appreciably in a few weeks. The same figure shows that, where a *moist* silicone grease is used, α' is much higher and, what is more, fairly constant.

Numerous experiments were also done with transistors whose envelopes contained, in addition to the silicone grease, a substance separately introduced as a water-vapour buffer. The buffer was either kept distinct from the grease by means of a porous plug (fig. 8*b*) or it was mixed with the grease. *Figs. 10a, b, c* and *d* give some examples of the favourable effect produced by some of these buffers (mentioned in the captions). The results in figs. 10*e* and *f* relate to transistors which contained, instead of a silicone grease, slightly moistened sand or silica gel, both of which substances serve the dual purpose of filler and buffer. These two examples support the hypothesis that the behaviour of the transistor is governed mainly by the moisture inside the enclosure, and not by the silicone grease or the combination of water and silicone grease.

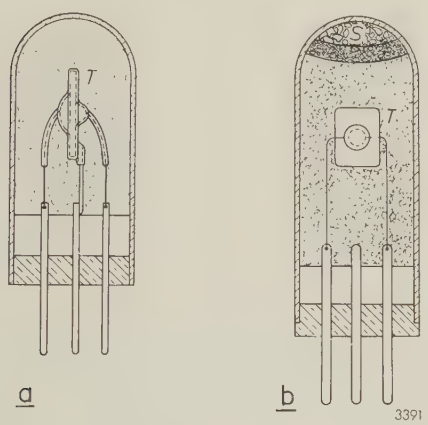

Fig. 8. *a*) Sketch of a transistor *T* in its envelope. The envelope is largely filled with a filler material (e.g. a silicone grease) to protect the germanium crystal during seal-off.
b) The envelope here contains a buffer or stabilizer *S*, separated from the silicone grease by a porous plug. At all temperatures the buffer produces a water-vapour pressure which keeps the water content of the germanium surface constantly favourable.

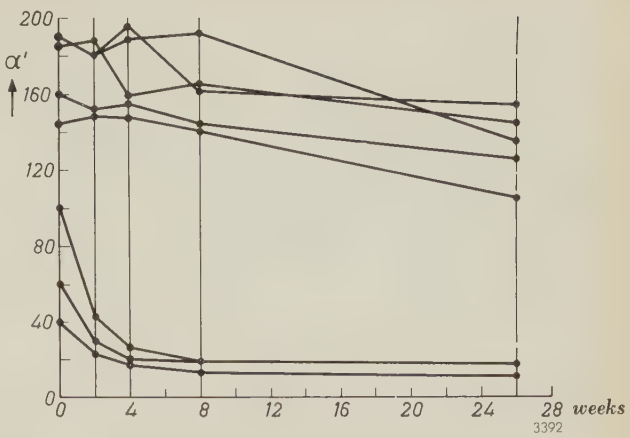

Fig. 9. Typical current amplification factor α' versus time after encapsulation in *dry* silicone grease (lower three curves) and in *moist* silicone grease (upper five curves). The ambient temperature during the experiments was 50 °C, and 50 mW was dissipated in the transistors. The temperature of the germanium crystal was 85 °C. The transistors used were *P-N-P* types, electrolytically etched in KOH. α' was measured at room temperature.

In fig. 10*f* it is noticeable that α' rises steeply during the first weeks, after which it remains roughly constant. We attribute this to the loss of water from the transistor surface when it is sealed into its envelope. Heat conduction through the electrodes then makes the crystal fairly hot, but the surroundings are kept cool, so that the water-vapour pressure remains low. After the seal-off, a low α' may therefore be expected. The surface water occupation is now out of equilibrium with the vapour pressure produced by the buffer, but at room temperature the equilibrium is restored only very slowly. If the transistor is operated, its temperature rises and the return to equilibrium is accelerated, which is apparent from changes in α'. If the transistor is kept at 100 °C, α' usually reaches its stable value after a few days. The transistors to which fig. 10*f* relates were not subjected to this pre-heating.

The temperature must not be raised above 100 °C with the object of speeding-up the above process. Experience has shown that higher temperatures, in conjunction with the high water-vapour pressure then produced by the buffers, inflict damage to the germanium surface, one result of which is a particularly low α'. Re-etching is then the only way to save the transistor.

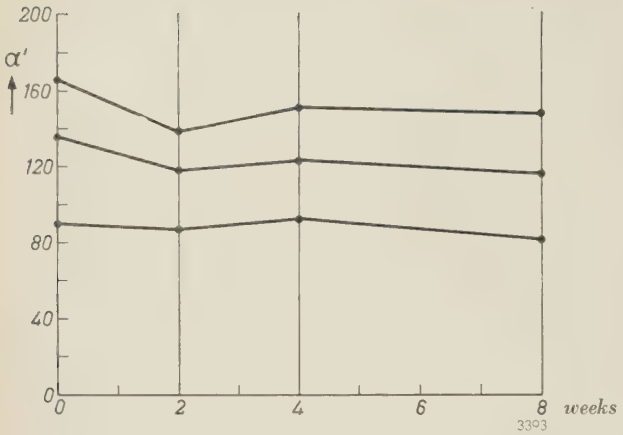

a) $BaCl_2.2aq$, separated from silicone grease (cf. fig. 8*b*).

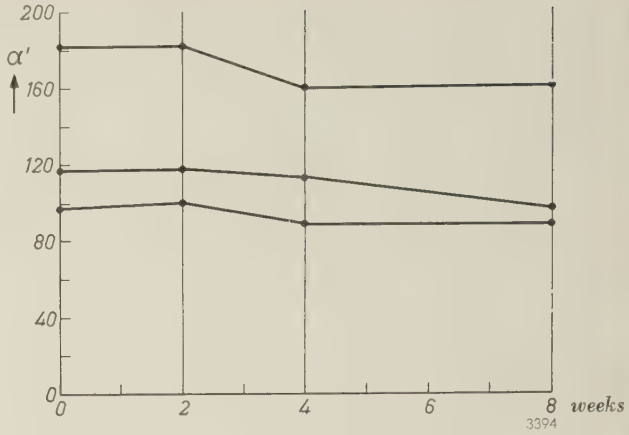

b) $K_2SO_4.NiSO_4.6aq$, separated from silicone grease.

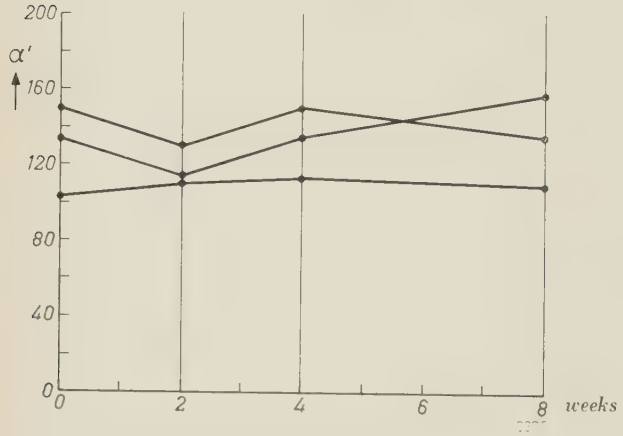

c) $K_2SO_4.Al_2(SO_4)_3.6aq$, mixed with silicone grease.

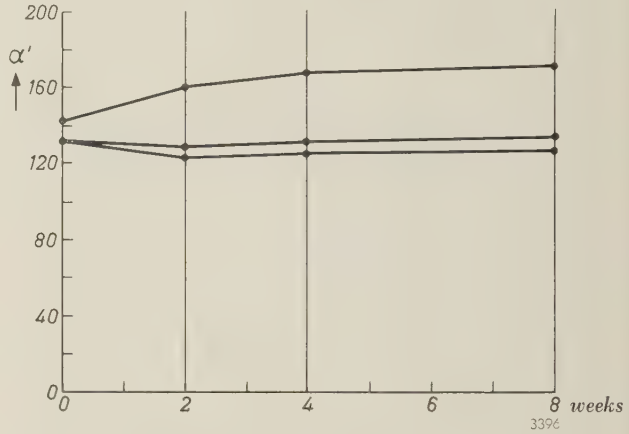

d) Boracic acid, mixed with silicone grease.

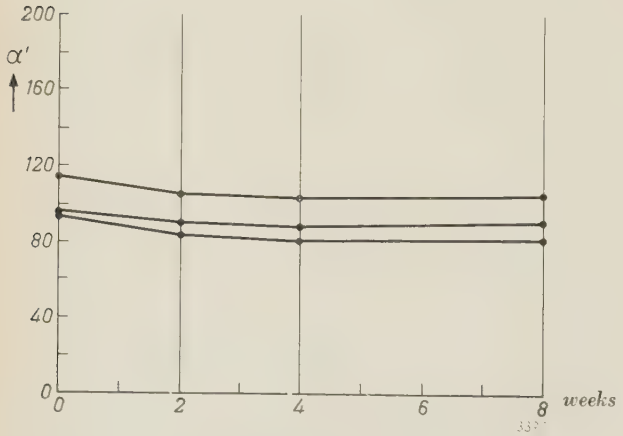

e) Slightly moist sand, serving also as filler material.

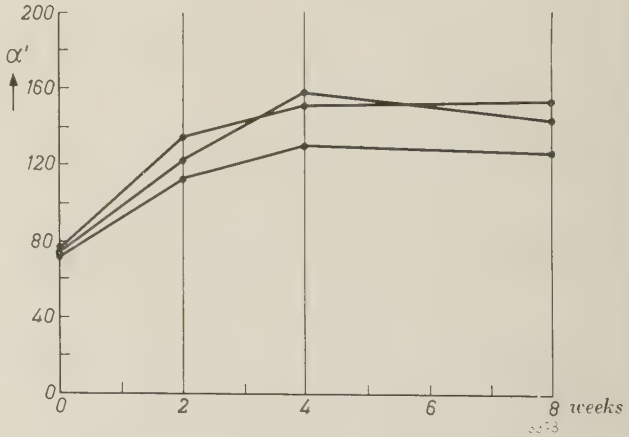

f) Silica gel, serving also as filler material.

Fig. 10. Examples of the behaviour of transistors with a buffer incorporated in the encapsulant to stabilize the water-vapour pressure. Ambient temperature 50 °C; dissipation 50 mW; temperature of germanium crystal 85 °C. α' was measured at room temperature. The curves relate to *P-N-P* transistors, electrolytically etched in KOH. The buffer used is mentioned below each graph. The level of α' is not characteristic of the buffer used.

Stabilization experiments by "forming" the surface

In order to stabilize transistors by "forming" their surface (p. 207), a buffer has to be introduced that gives a lower water-vapour pressure than is required for normal stabilizing. We have achieved successful results with transistor fillings consisting of a silicone grease mixed with a little boracic acid (say 5% by weight), from which water is expelled to the required degree by drying. If the encapsulated transistors are formed by heating them for three days at 140 °C,

stable transistors are produced which possess favourable properties in every respect. *Fig. 11* demonstrates the stability of α' after weeks of continuous loading; *fig. 12* represents α' as a function of the time of storage at 100 °C.

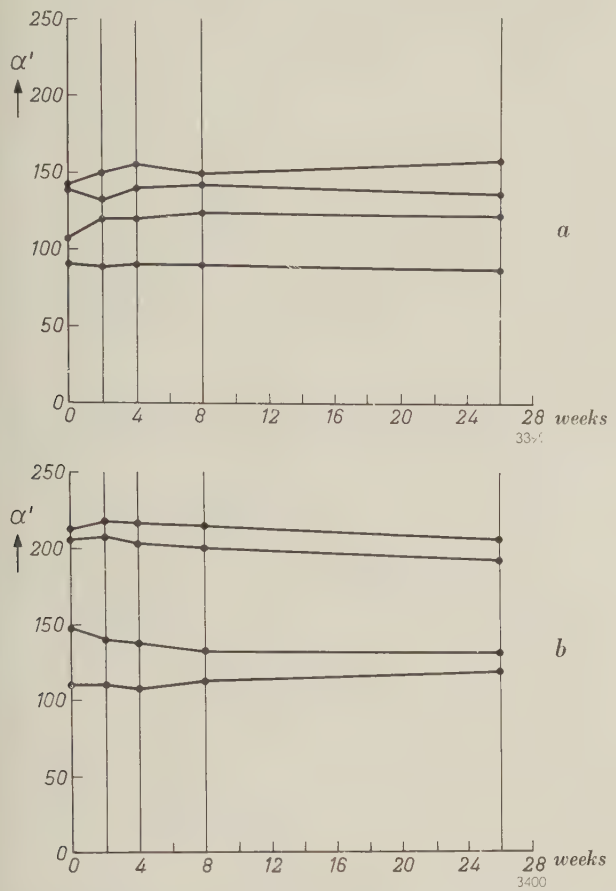

Fig. 11. Examples of the behaviour of α' in life tests on transistors stabilized by surface forming at 140 °C. Buffer 5% pre-heated boracic acid, mixed with silicone grease. Dissipation 50 mW (5 mA, 10 V). Ambient temperature 50 °C, the temperature of the crystal then being 85 °C. α' was measured at room temperature. (The level of α' is not characteristic of the stabilizing method or of the type of transistor.)
a) *P-N-P* transistors.
b) *N-P-N* transistors.

It is particularly important to extend the forming process over a sufficiently long period of time. It is seen from *fig. 13* that α', as expected, is low immediately after encapsulation. After heating at 140 °C for one day, its value has increased considerably, but there is again a sharp drop after storing the transistor for a day at room temperature. The forming process was too short. After prolonged heating at 140 °C (here 6 days), however, the improvement achieved is not lost again. But the forming should not be too prolonged, otherwise α' begins to fall once more.

Longer forming is required, or a higher forming temperature, the lower is the vapour-pressure curve of the buffer. This is illustrated in *fig. 14*, which relates to a transistor whose envelope was filled with a silicone grease mixed with boracic acid, which had been dried out more than in the cases earlier discussed. In practice the mixture of silicone grease and boracic acid will be chosen with a view to limiting the forming process to a few days of heating at 140 °C. A higher temperature is undesirable, since the indium in the collector and emitter melts at about 155 °C.

It is likely that during the forming process — and perhaps afterwards — the silicone grease in combination with the boracic acid has its own advantageous effect. At the forming temperature there may well be reactions between the grease and the boron compounds which favourably influence the transistor's characteristics. However, that water vapour plays the major role in the forming process appears from the fact that transistors with very low values of α' are obtained when a drying agent, e.g. barium oxide, is added inside the envelope.

The method of stabilization by forming the surface in a mixture of silicone grease and boracic acid not only produces high and stable values of α', but also benefits other important transistor characteristics (*Table I*). For example, the saturation leakage currents at the *P-N* junctions are small and do not drift. This is in contrast with the leakage currents in many commonly used transistors, which may gradually assume appreciable values, particularly if the temperature of the transistor is relatively

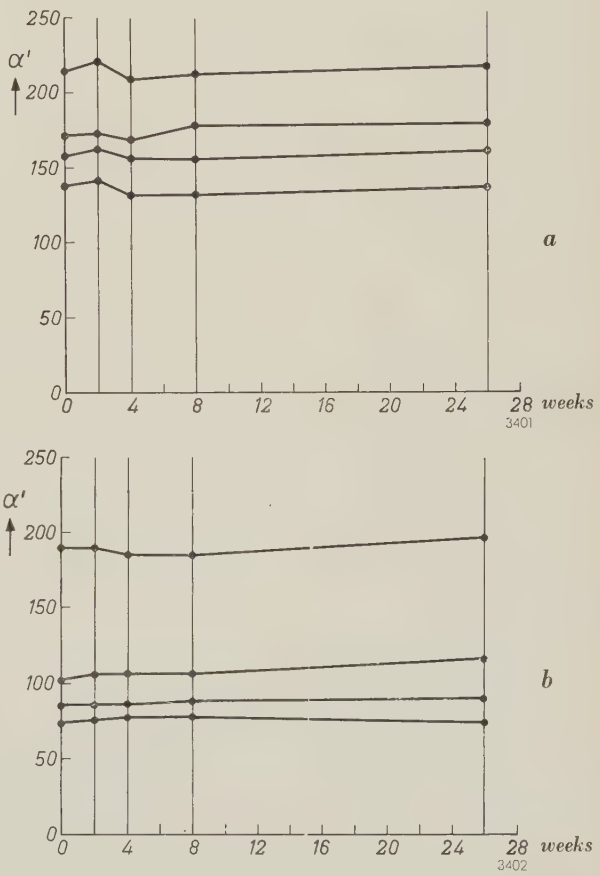

Fig. 12. Examples of the behaviour of α' in storage tests at 100 °C on transistors stabilized by forming. Buffer 5% preheated boracic acid, mixed with silicone grease. α' was measured at room temperature. (The level of α' is not characteristic of the stabilizing method or of the type of transistor.)
a) *P-N-P* transistors.
b) *N-P-N* transistors.

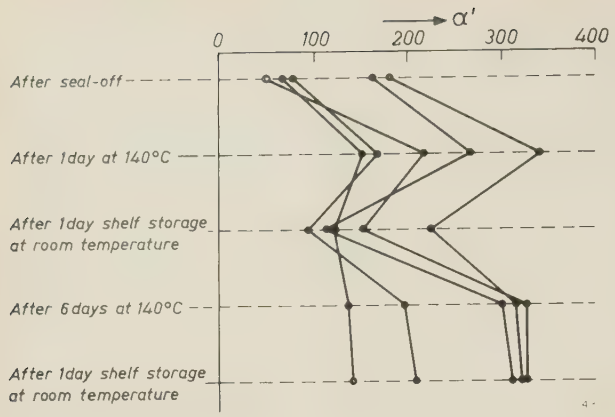

Fig. 13. Variation of α' of some P-N-P transistors, electrolytically etched in KOH, which were initially formed for too short a time (one day) and subsequently for a long enough time (six days). α' was measured at room temperature.

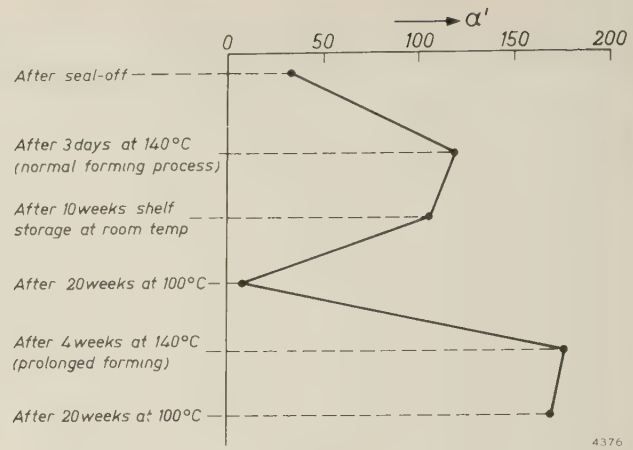

Fig. 14. Variation of α' of a transistor formed with a buffer giving a considerably lower water-vapour pressure than in the cases to which figs. 11, 12 and 13, and Table I, refer. α' was measured at room temperature.

Table I. The current amplification factor α', the saturation leakage currents I_{C_0} at the collector junction and I_{E_0} at the emitter junction, and the noise, of representative examples of P-N-P and N-P-N transistors, after various successive treatments. The transistor envelopes were filled with a silicone grease mixed with 5% boracic acid, dehydrated to a certain degree by pre-drying. The measurements were done at room temperature.

	P-N-P				N-P-N			
	α'	I_{C_0} (μA)	I_{E_0} (μA)	Noise (dB)	α'	I_{C_0} (μA)	I_{E_0} (μA)	Noise (dB)
After electrolytic etching in KOH	210	8	6	—	89	0.6	0.6	—
After seal-off	56	26	22	—	40	1.3	1.2	—
After 1 day at 100 °C	75	—	—	—	68	—	—	—
After 24 hrs storage at room temperature	60	2.8	2.7	4	53	4.4	3.5	6
After 3 days at 140 °C (forming)	158	—	—	—	164	—	—	—
After 24 hrs storage at room temperature	158	1.8	1.6	4	172	0.3	0.2	4

high (e.g. 60 °C). The table further shows that the noise level, which is often correlated with the leakage currents, is also favourable in formed transistors. In fact, the noise values found are just about the lowest yet measured on transistors.

In the case of P-N-P transistors the breakdown potentials of the two P-N junctions after forming are generally 20 to 30% lower than before. The breakdown potentials in N-P-N transistors are not significantly affected.

Finally it should be noted that surface forming also has a fairly marked influence on the I_E-V_{EB} characteristic (*fig. 15*).

Stabilizing with arsenic

Water is not alone in its property of reducing the recombination of holes and electrons at the germanium surface. Another substance with which we have successfully experimented is arsenic. At first sight there would seem to be no relation between water and arsenic, and the reader may well wonder how it happened to be chosen for experiments at all. It is not really so odd, however. Extensive physico-chemical investigations into the influence exerted by water on the surface of semiconductors have revealed that water adhering to such a surface tends to induce N-type surface conductivity. On N-type germanium, water thus makes the surface layer more strongly N-type than the interior, and on P-type germanium it makes the surface layer less strongly P-type than the interior. It may even result in an N-type surface layer on germanium that is only weakly P-type [7]). The question arose whether donor elements like arsenic, phosphorus, antimony and bismuth, with which germanium is doped to induce N-type conductivity, might have a similar effect on the germanium surface as water has. This proved indeed to be the case, particularly as regards arsenic and phosphorus, which have measurable vapour pressures at 140 °C.

[7]) R. H. Kingston, Water-vapor-induced N-type surface conductivity on P-type germanium, Phys. Rev. **98**, 1766-1775, 1955.

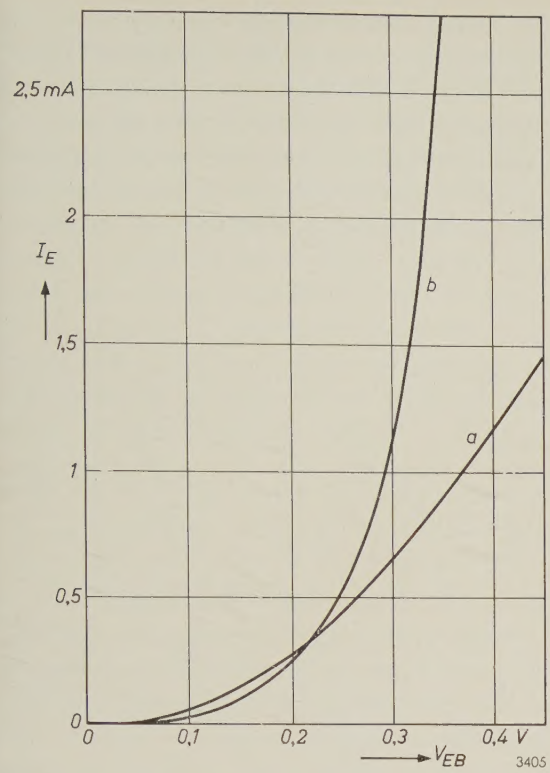

Fig. 15. Illustrating the effect of forming on the I_E-V_{EB} characteristic of a *P-N-P* transistor; *a*) before forming, *b*) after forming.

We shall only comment briefly on the stabilizing method whereby a dried silicone grease mixed with a few percent by weight of arsenic powder is used as the filler substance in transistor envelopes. In its effect this mixture closely resembles the mixture of silicone grease and boracic acid used for the transistors stabilized by surface forming with water vapour. Again, a forming period of several days at 140 °C or higher is necessary. The resulting transistors have a high α' and excellent stability (*fig. 16*). In fact, in many aging tests, α' showed no change whatsoever.

It is not to be expected that the arsenic at 140 °C will really diffuse in the germanium surface layer and be incorporated in the germanium lattice as donor impurities normally are. For any significant diffusion to occur, the temperature would have to be at least 600 °C. Experiments have proved that the arsenic nevertheless gives rise to a surface layer which is strongly *N*-type. This layer persists as long as the transistor together with the arsenic is hermetically sealed. If the transistor is exposed to the ambient air, the surface layer changes and the transistor is no longer stable. The effect of the arsenic is entirely destroyed if the transistor is introduced into a space which is evacuated at high temperature. Evidently the arsenic is bound only very weakly to the germanium surface.

An advantage over the forming method using a silicone grease and boracic acid is that the transistors obtained are much more capable of withstanding high temperatures. Arsenically treated transistors can be held, for example, at a forming temperature of 140 °C for several months without deteriorating, whereas the same treatment with silicone grease and boracic acid would result in a considerable drop in α'.

A complication is that transistors etched in KOH and subsequently formed with arsenic exhibit a marked "shelf after-effect". When such transistors, after a period of storage at room temperature, are raised to a higher temperature, α' gradually rises for a few days. When the transistors are then returned to room temperature, α' again declines, at

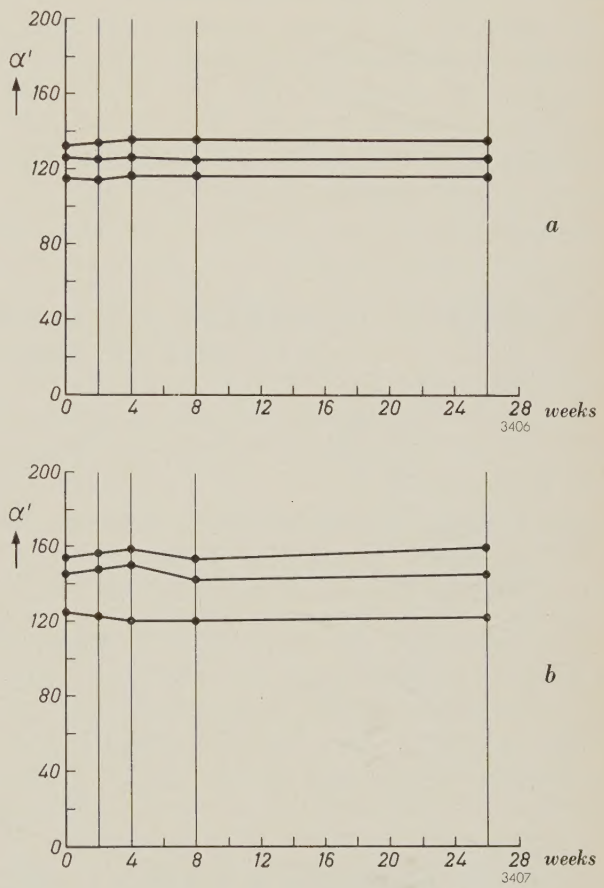

Fig. 16. Some examples of the constancy of α' of transistors formed with arsenic. Before each measurement of α', the transistor was shelf-stored at room temperature for 24 hours.
a) During operation; dissipation 50 mW, ambient temperature 50 °C.
b) Stored, at 140 °C.

first rapidly and then slowly (*fig. 17*). It may be a month before the original value is reached. This effect is not found on transistors formed with a silicone grease and boracic acid mixture. The effect is apparently bound up with the presence of traces

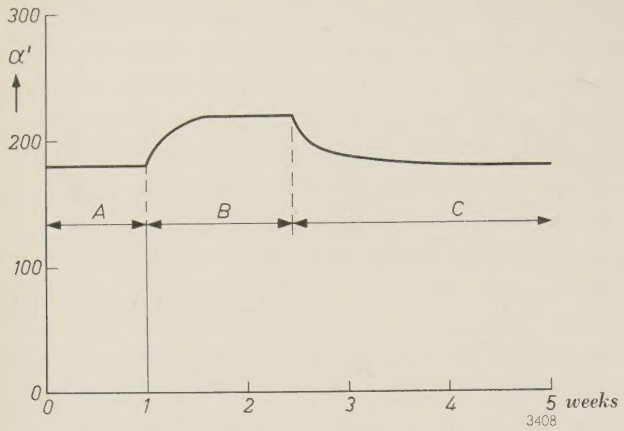

Fig. 17. Transistors formed at 140 °C, with powdered arsenic mixed in the silicone grease, often show a marked "shelf after-effect".
Period *A*: transistor at room temperature.
Period *B*: transistor at 100 °C.
Period *C*: transistor at room temperature.

of water in the transistor envelope, since if the transistors are rigorously dried after forming (by enclosing a drying agent in the envelope), the result is a high and stable α' without this shelf after-effect.

A simpler way of eliminating the effect is to mix boracic acid as well as arsenic with the grease. This is the procedure with which we have so far achieved the best results. The transistors so treated combine the advantages of boracic-acid and arsenic forming, namely no shelf after-effect, high and very constant value of α' and high temperature stability.

Summary. The surface state of germanium transistors has a very marked influence on their characteristics, in particular on the current amplification factor. The occupation of the surface by water molecules is shown to be exceptionally important, and is thought to have an optimum value. A favourable water occupation may be maintained in all operating conditions by incorporating in the encapsulant a buffer substance — a stabilizer — which provides the appropriate water-vapour pressure as a function of temperature. Whilst this method produces good transistors with reasonably stable characteristics, better results are obtained with a buffer whose water-vapour pressure is initially too low. After the transistors have been heated for several days, they are then found to have very favourable and stable characteristics. The process is described as "surface forming". There are other substances that resemble water in their effect on the surface. Results obtained with one such substance (arsenic) are briefly discussed.

ABSTRACTS OF RECENT SCIENTIFIC PUBLICATIONS BY THE STAFF OF N.V. PHILIPS' GLOEILAMPENFABRIEKEN

Reprints of these papers not marked with an asterisk * can be obtained free of charge upon application to Philips' Electrical Ltd., Century House, Shaftesbury Avenue, London W.C. 2, where a limited number of reprints are available for distribution.

2780: S. Duinker: General energy relations for parametric amplifying devices (T. Ned. Radiogenootschap **24**, 287-310, 1959, No. 5).

It is shown that the energy relations pertaining to parametric amplifying devices, as they have been derived by various authors, are a direct consequence of the invariance of the total-energy function of the parametric system under certain transformations. The theory is generalized so as to comprise arbitrary parametric systems. Some general properties of parametric systems, which can be deduced immediately from the energy relations, are discussed. A small number of typical examples are briefly treated to illustrate some fundamental principles following from the general theory.

2781: W. Albers and J. T. G. Overbeek: Stability of emulsions of water in oil, I. The correlation between electrokinetic potential and stability (J. Colloid Sci. **14**, 501-509, 1959, No. 5).

Experiments on water-in-oil emulsions of moderate concentration, stabilized with oil-soluble, ionizing stabilizers, show that in these emulsions no correlation exists between stability against flocculation and electrokinetic potential. Although, according to theoretical calculations, energy barriers of over 15 kT are present if the radius of the dispersed globules is about 1 μ and the electrokinetic potential exceeds 25 mV, they apparently do not prevent lasting contact between particles. All the emulsions flocculate rapidly, even in the presence of a surface potential considerably higher than 25 mV. A rather pronounced anticorrelation exists between the zeta potential and coalescence. It is explained as a consequence of the free mobility of the stabilizing molecules in the interface. The good stabilization against coalescence caused by some oleates of polyvalent metals is due to the formation of a thick film of partial hydrolyzates in the interface.

2782: W. Albers and J. T. G. Overbeek: Stability of emulsions of water in oil, II. Charge as a factor of stabilization against flocculation (J. Colloid Sci. **14**, 510-518, 1959, No. 5).

It is shown by theoretical calculations that the energy barrier between charged droplets in water-in-oil emulsions is strongly diminished when the concentration of the emulsion is not extremely low. This is a consequence of the great extension of the diffuse electrical double layer in oil. The high concentration in the sediment (or cream) therefore strongly promotes flocculation. Gravity also promotes flocculation directly in all but the most dilute water-in-oil emulsions because the weight of the particles in higher layers transmitted by the extended double layers presses on those in the lower layers and forces them together.

2783: F. N. Hooge: Influence of bond character on the relation between dielectric constant and refraction index (Z. phys. Chemie (Frankfurt a.M.) **21**, 298-301, 1959, No. 3/4).

In the relation given by Szigeti relating the dielectric constant of cubic ionic compounds with the refractive index, it is shown that the value of the experimental constant s depends on the bond character obtaining in the crystal. Using Pauling's model it is shown that s may be calculated from quantities that determine the bond character of a crystal.

2784: G. Diemer and J. G. van Santen: Nieuwe toepassingen van elektro-optische verschijnselen (Ned. T. Natuurk. **25**, 265-287, 1959, No. 10). (New applications of electro-optical phenomena; in Dutch.)

A survey is given of the fundamental properties and possible applications of electroluminescence, photoconduction and combinations in the fields of image intensification, image display, radiation detection, electric amplification and logic, switch and memory devices.

2785: T. J. de Man and J. R. Roborgh: The hypercalcemic activity of dihydrotachysterol$_2$ and dihydrotachysterol$_3$ and of the vitamins D_2 and D_3; comparative experiments on rats (Biochem. Pharmacology **2**, 1-6, 1959, No. 1).

The hypercalcemic activities of dihydrotachysterol$_2$, dihydrotachysterol$_3$, vitamin D_2 and vitamin D_3 have been compared at different intervals (2, 4, 7 and in some cases 1 and 10 days) after the administration to rats of one oral dose of the crystalline compounds in pure peanut oil. The maximal serum calcium levels appear to be obtained 2-4 days after the administration. From the results it appears that dihydrotachysterol$_3$ is the most active hypercalcemic agent, followed, in decreasing order, by dihydrotachysterol$_2$, vitamin D_3 and vitamin D_2. The activity ratios proved to be highly dependent on the time interval. As to the hypercalcemic activity, the potency ratio vitamin D_3/vitamin D_2 has been found to be about 1.6, while, with respect to their antirachitic activities, both vitamins are equipotent in rats. The antirachitic activity of dihydrotachysterol$_3$ was shown to be nearly twice as high as the potency of dihydrotachysterol$_2$, the antirachitic activity of dihydrotachysterol$_2$ being about 0.5 per cent of the vitamin D_3 activity.

2786: J. H. Uhlenbroek and J. D. Bijloo: Isolation and structure of a nematicidal principle occurring in Tagetes roots (Proc. 4th int. Congr. Crop Protection, Hamburg 1957, Vol. 1, pp. 579-581; published 1959).

Note and discussion concerning extraction and structure of a nematicidal principle from Tagetes roots.

2787: J. Meltzer and F. C. Dietvorst: Relation between chemical structure and ovicidal and leaf-penetrating properties of some new acaricides (Proc. 4th int. Congr. Crop Protection, Hamburg 1957, Vol 1, pp. 669-673; published 1959).

Sulphur-linked diphenyl compounds possess high acaricidal activity. The sulphone ("Tedion"), sulphoxide and sulphide homologues of the 2,4,5,4′-tetrachloro-derivatives do not differ greatly in ovicidal and larvicidal activity. Direct contact action on the eggs, however, is stronger with the sulphone and least with the sulphide. Leaf penetration is fastest for the sulphide and slowest for the sulphone. As regards residual action, the sulphone is appreciably longer lasting than the sulphoxide and the sulphide. p-chlorophenyl benzenesulphonate and chlorbenside show a faster leaf penetration than Tedion, and in consequence a shorter residual action.

2788: J. Rodrigues de Miranda and H. van den Kerckhoff: Designing a multi-purpose stereo pre-amplifier (J. Audio Engng. Soc. **7**, 75-80, 1959, No. 2).

In between the required sensitivity and the required output voltage the stereo pre-amplifier should be designed with a good tone and volume control system. Logical design leads to a pre-amplifier with distortion as low as 0.03% for all frequencies. Included in the design is a simple but effective rumble filter.

2789: J. L. Ooms and C. R. Bastiaans: Some thoughts on geometric conditions in the cutting and playing of stereodiscs and their influence on the final sound picture (J. Audio Engng. Soc. **7**, 115-121, 1959, No. 3).

The influence of various geometric conditions in the cutting and reproducing process is investigated. It is found that stylus contour plays no important role. Axis orientation does play a role; any deviation herein causes cross modulation, ultimately leading to distortion of the original stereophonic sound picture. Slant and rotation of planes of axes may be disregarded since the resultant difference angles are small enough to be neglected. Finally, the nature of sound-picture distortion caused by such cross modulation is investigated. Amplitude distortion leads to angular shift of the sound sources (panorama distortion), phase relationship of cross-modulation components causing increase or decrease in width of the sound picture (basis distortion).

2790: J. L. Meijering: Thermodynamical calculation of phase diagrams (The physical chemistry of metallic solutions and intermetallic compounds, Proc. Symp. Nat. Phys. Lab., June 1958, Vol. 2, paper No. 5 A).

Survey article outlining the methods and limitations of thermodynamics for the prediction and extrapolation of phase diagrams. The subject matter is treated under the following headings: binary miscibility gaps, solid-liquid equilibria, ferrite-austenite equilibria, ternary miscibility gaps. About 50 references are given to the original literature.

2791: G. Meijer: Photomorphogenesis in different spectral regions (Proc. Conf. Photoperiodism and related phenomena in plants and animals, Gatlinburg, Tennessee, Oct.-Nov. 1957, edited by R. Withrow, pp. 101-109; published 1959).

In experiments with some photoperiodically-sensitive plants it is shown that for obtaining a long-day effect two different photo reactions are involved, a red-sensitive one which can be reversed by near infrared, and a blue/near-infrared sensitive reaction. The elongation of internodes is inhibited by light. Two inhibiting processes were distinguished, one occurring in red light and being antagonized by near infrared, the other one occurring in blue light. With a certain intensity it was found that it depends on the plant species which process predominates.

2792: W. Verweij: Probe measurements in the positive column of low-pressure mercury-argon discharges (Physica **25**, 980-987, 1959, No. 10).

In the positive column of electric discharges in mixtures of argon and mercury vapour at low pressure, electron concentration, electron temperature and axial field strength are determined with the aid of Langmuir probes. The mercury pressure is varied from 0.50×10^{-3} mm Hg to 90×10^{-3} mm Hg, the argon pressure from 0 to 20 mm Hg and the mean current density from 10 mA/cm^2 to 80 mA/cm^2. If very thin cylindrical probes (20 μ diameter) are used, the measurements of the electron concentration based on plasma potential and those found from the characteristic at positive probe voltage are in very good agreement. For the discharges under examination, the mobility of the electrons is evaluated from the electron concentration, the electron gradient and the tube current.